

# A semi-supervised framework for diverse multiple hypothesis testing scenarios

Jack Freestone<sup>1\*</sup>, William Stafford Noble<sup>2,3</sup>, and Uri Keich<sup>1\*</sup>

<sup>1</sup>School of Mathematics and Statistics F07, University of Sydney

<sup>2</sup>Department of Genome Sciences, University of Washington

<sup>3</sup>Paul G. Allen School of Computer Science and Engineering, University of Washington

\*Corresponding authors: J.Freestone@maths.usyd.edu.au, uri.keich@sydney.edu.au

## Abstract

Standard multiple testing procedures are designed to report a list of discoveries, or suspected false null hypotheses, given the hypotheses' p-values or test scores. Recently there has been a growing interest in enhancing such procedures by combining additional information with the primary p-value or score. Specifically, such so-called side information can be leveraged to improve the separation between true and false nulls along additional dimensions thereby increasing the overall sensitivity. In line with this idea, we develop RESET (REScoring via Estimating and Training), which uses a unique data-splitting protocol that subsequently allows any semi-supervised learning approach to factor in the available side information while maintaining finite-sample error rate control. Our practical implementation, RESET Ensemble, selects from an ensemble of classification algorithms so that it is compatible with a range of multiple testing scenarios without the need for the user to select the appropriate one. We apply RESET to both p-value and competition based multiple testing problems and show that RESET is (1) power-wise competitive, (2) fast compared to most tools and (3) able to uniquely achieve finite sample false discovery rate or false discovery proportion control, depending on the user's preference.

# 1 Introduction

Scientists are often interested in testing many null hypotheses,  $\{H_i : i = 1, \dots, m\}$ . As an example, a scientist may be interested in assessing which genes exhibit a change in gene expression levels in response to a particular drug treatment. In this case, the  $i$ th null hypothesis  $H_i$  states that ‘the  $i$ th gene exhibits no change in gene expression level’. This type of large-scale hypothesis testing is usually achieved by assigning a p-value,  $p_i$ , to each null hypothesis. The collection of p-values then undergoes a filtering process that rejects a subset of these null hypotheses that have sufficiently small p-values subject to a type-1 error rate control to minimize the number of misreported true null hypotheses.

The most common choice of error rate in this setup is the false discovery rate (FDR), which is defined as the expectation of the false discovery proportion (FDP) — the fraction of true null hypotheses in the reported list of rejections, or *discoveries* [2]. In this case, the filtering procedure ensures that the FDR is  $\leq \alpha$  where  $\alpha \in (0, 1)$  is a prespecified threshold. Alternatively, we might be interested in controlling the FDP rather than its expectation in the following sense. Given a confidence parameter  $\gamma$  and a threshold  $\alpha$ , the FDP is said to be controlled if  $\mathbb{P}(FDP > \alpha) \leq \gamma$ . Evidently, such FDP control reduces the risk that the realized FDP exceeds  $\alpha$ , which is not guaranteed by FDR control [16, 19, 20, 27, 38, 40].

Determining a p-value for each null hypothesis can be challenging because (a) it requires knowledge of the underlying null distribution and (b) it can be computationally intensive. A recently developed competition framework offers an alternative approach to FDP/FDR control that does not require computation of canonical p-values [1, 21]. Instead, all that these procedures require is a single draw,  $\tilde{Z}_i$ , from each null distribution. The null drawn  $\tilde{Z}_i$  is then compared with  $Z_i$ , the originally observed score (test statistic) for  $H_i$ , thus conceptually providing a crude 1-bit p-value.

These p-values are too crude to be used in typical p-value based filters. Instead, assuming that larger values of  $Z_i$  provide more evidence against  $H_i$ , we compare each pair of scores  $(Z_i, \tilde{Z}_i)$  by recording a label  $L_i \in \{\pm 1\}$  indicating which was the largest of the two scores, as well as a winning score,  $W_i = f(Z_i, \tilde{Z}_i)$ . The function  $f$  needs to be symmetric in its arguments and should increase with the values of  $Z_i$  and  $\tilde{Z}_i$ , e.g.,  $W_i = Z_i \vee \tilde{Z}_i$ , or with the discrepancy between the two, e.g.,  $W_i = |Z_i - \tilde{Z}_i|$ .<sup>1</sup> For each true null hypothesis,  $L_i$  is equally likely to be  $\pm 1$  independent of all the scores  $W = \{W_i\}$  and all other labels  $L_{-i}$  because both scores were sampled from the same null distribution and  $f$  is symmetric. Hence, the number of negative labels, those with  $L_i = -1$ , can be used to estimate the number of true nulls with positive labels among the top scoring hypotheses. Using this fact, the labels and scores  $\{(L_i, W_i) : i = 1, \dots, m\}$  are passed through a filter to reject a subset of the top scoring hypotheses, with either the FDR or FDP controlled depending on the user’s preference.

More recently, research has been focused on improving these filtering methods by leveraging side information  $\mathbf{x}_i \in \mathcal{X}$  that complements each p-value  $p_i$  or score  $W_i$  to better discriminate between the true and false null hypotheses. These methods utilize a variety of strategies but ultimately operate with the same goal in mind: the side information is used to weight or rescore the hypotheses according to how confidently we believe that each hypothesis is a false null. Indeed, there are several such tools that augment p-values with side information [25, 33–35, 37, 51]. When it comes to using side information in the competition framework, we are aware of only one fully specified method with rigorous error-rate control, which is the recently published Adaptive Knockoffs [44] (AdaPT [33] only offers a meta-procedure).

In this paper, we offer a novel approach for multiple testing with side information. The idea

---

<sup>1</sup>In general, the functions can be hypothesis-dependent, i.e.,  $f_i$  instead of  $f$ .

is to randomly split a set of suspected true nulls into two sets, where one set is used for training a semi-supervised learning model to discriminate between the true and false null hypotheses, and the other for estimating the number of false discoveries. Accordingly, we refer to our new approach as *RESET*—REScoring via Estimating and Training. Our method flexibly incorporates any semi-supervised approach to help distinguish between true and false null hypotheses. Moreover, it is equally applicable to the competition and p-value context and allows the user to choose between FDR or FDP control. We evaluate RESET in a range of simulations and real data applications to verify that it is a competitive alternative to existing methods in terms of statistical power and speed.

## 2 Background: competition-based multiple testing

Competition-based multiple testing was first established in the proteomics community where the goal is to infer which proteins, i.e., long chains of amino acids, are present in a biological sample [17]. Direct protein detection is challenging, and so a bottom-up approach is taken where the proteins are broken into small chains of amino acids, called *peptides*, and the objective is to identify these peptides instead. Then, a process called *liquid chromatography tandem mass spectrometry* (LC-MS/MS) is used to isolate each sample peptide and subsequently generate a fragmentation spectrum. Each such spectrum can be thought of as a fingerprint of the peptide that generated the spectrum, allowing us to hypothesize which peptides are present in the sample.

This is done by searching each spectrum against a database of candidate peptides called *targets* to find the spectrum’s optimal peptide-spectrum match (PSM), along with a score indicating the strength of the match. Unfortunately, due to the incomplete nature of the database and the noise associated with generating the spectra, the PSM can be incorrect. Hence, we wish to employ a testing procedure for each null hypothesis  $H_i$  that ‘the  $i$ th target is not present in the sample’. In order to decide which null hypotheses to reject, we pair each target peptide with a *decoy* peptide that is generated by randomly shuffling or reversing the target peptide’s sequence. Accordingly, a second search is performed for each spectrum against the database of decoys to obtain a second PSM and associated score, and only the highest scoring PSM out of the two is retained.

As outlined in the introduction, we accompany  $H_i$  with a score  $Z_i$ , defined as the maximum scoring PSM associated with the  $i$ th target peptide, and the higher the score, the more likely  $H_i$  is false, i.e., the peptide is in the sample. Similarly, we define  $\tilde{Z}_i$  as the maximum scoring PSM associated to the  $i$ th target’s corresponding decoy peptide. For each true null hypothesis, we expect  $Z_i$  and  $\tilde{Z}_i$  to be drawn from the same (hypothesis-specific) null distribution, independently of everything else. Finally, we obtain a winning score  $W_i = Z_i \vee \tilde{Z}_i$  and a label  $L_i$  indicating whether the winning score was from the  $i$ th target or its decoy [42].

Subsequently, the statistics community independently formalized this idea in the context of variable selection, where the goal is to identify relevant variables from  $\{X_i : i = 1, \dots, p\}$  that are associated with a response  $y$ . The procedure that achieves this while controlling the FDR is called the *knockoff filter*, which begins by pairing each variable  $X_i$  with an artificial variable  $\tilde{X}_i$ , called a *knockoff*. In this paper, we consider the *model-X* version of the knockoff filter [7] which makes the following assumptions<sup>2</sup>. First, the joint distribution of the variables,  $X$ , is assumed to be known. Second, each observation  $(X_{i,1}, \dots, X_{i,p}, y_i)$  is sampled *i.i.d.* from the joint distribution  $F_{XY}$ . Because  $X$  is random and its distribution known, the knockoffs  $\tilde{X}$  are also constructed randomly subject to the following conditions:

---

<sup>2</sup>However, our results are equally applicable to the *fixed-X* model as well [1].

1. The joint distribution of  $\hat{X} := [X, \tilde{X}]$  is the same if we swap a subset of the variables and their corresponding knockoffs, i.e.,  $\hat{X} \circ \Pi \stackrel{d}{=} \hat{X}$ , where  $\Pi$  is a permutation that swaps the subset of variable indices for their corresponding knockoff indices.
2. We construct  $\tilde{X}$  independently of  $y$  by only looking at  $X$ , i.e.,  $\tilde{X} \perp\!\!\!\perp y \mid X$ .

Once the knockoffs have been constructed, each variable is given a user-defined score  $W_i := W_i([X, \tilde{X}], y) \in \mathbb{R}$  and a label  $L_i([X, \tilde{X}], y) \in \{\pm 1\}$ . The idea is that the label  $L_i$  indicates whether the variable  $X_i$  or the knockoff  $\tilde{X}_i$  has greater evidence for being relevant to the model, and the score  $W_i$  indicates by how much. Commonly, the score and label are combined by setting  $\text{sign}(W_i) = L_i$ ; however, as will become clear in our later presentation of RESET, it is instructive to separate them.

In this paper, we consider the *Lasso Coefficient Difference* (LCD) score, which is the difference in the magnitude of the coefficients of the Lasso regression [49]. Specifically, cross-validation is used to determine the  $\lambda$  penalty when regressing on the augmented design matrix  $[X, \tilde{X}]$ . We denote the absolute values of the Lasso( $\lambda$ )-fitted coefficients as  $Z_i$  for the variables and  $\tilde{Z}_i$  for the knockoffs. The scores and labels are then defined as

$$W_i := |Z_i - \tilde{Z}_i|, \quad L_i := \text{sign}(Z_i - \tilde{Z}_i). \quad (1)$$

Hypotheses with zero scores are typically ignored. In either context, peptide inference or variable selection, we expect that the labels of the true null hypotheses are independently and equally likely to be  $\pm 1$ , independently of everything else. This is formalized in the next assumption.

**Assumption 1.** *Let  $N$  be the indices of the true null hypotheses. The labels  $\{L_i : i \in N\}$  are i.i.d.  $\pm 1$  uniform random variables independent of all the scores  $W$  and the labels of the false null hypotheses.*

For the knockoff filter, Assumption 1 follows from the knockoff construction, whereas in the peptide detection problem, Assumption 1 is based on our previous discussion that the scores of a null target and its decoy,  $Z_i$  and  $\tilde{Z}_i$ , are independent draws from the same null distribution, and moreover, this happens independently of all other pairs of scores. This assumption is commonly applied in the literature, with several analyses validating this claim empirically [21, 39].

Given the above assumption, the number of hypotheses with  $L_i = -1$  (i.e., decoy or knockoff wins) that score above a score cutoff of  $\tau$  can be used to estimate the number of true null hypotheses that score above  $\tau$  with  $L_i = 1$ . Using this strategy, we can report a list of discoveries while satisfying a type-1 error rate control in one of two ways. The first and by far the more common way is to apply *Selective SeqStep+* (SSS+) [1], which controls the FDR at a prespecified threshold  $\alpha$  by reporting the following list of discoveries  $R_\alpha$ :

$$R_\alpha := \{i \in [p] : W_i \geq \tau, L_i = 1\}, \quad \text{where } \tau := \min \left\{ t \in \mathbb{R} : \frac{\#\{W_i \geq t, L_i = -1\} + 1}{\#\{W_i \geq t, L_i = 1\} \vee 1} \leq \alpha \right\}. \quad (2)$$

SSS+ is made precise in Algorithm S1 and works in a more general setting when the probabilities of the positive and negative labels of the true null hypotheses are no longer uniform, i.e.,  $\mathbb{P}(L_i = 1) = c$  and  $\mathbb{P}(L_i = -1) = 1 - c$ . In the proteomics community, the application of Equation (2) in the peptide detection problem is referred to as *target-decoy competition* or TDC for short. As such, we will refer to the method as TDC in the peptide detection setting, and SSS+ in the variable selection setting and more generally.

Alternatively, we can control the FDP by using, for example, *FDP-stepdown* (FDP-SD, Algorithm S2) [40]. FDP-SD works by first reranking the labels  $L$  according to the scores  $W$  in

descending order. Next, it compares the number of decoy (knockoff) wins in the first  $i$  hypotheses, denoted as  $D_i := \#\{L_j = -1 : j \leq i\}$ , with a precomputed bound  $\delta_i$ , which is determined by  $\alpha$  and  $\gamma$ . Each comparison is made in a ‘stepdown’ fashion, i.e., if the first  $i$  hypotheses satisfy  $D_1 \leq \delta_1, \dots, D_i \leq \delta_i$ , then it moves on to the next comparison at  $i + 1$ . For small  $i$ , it is impossible for  $D_i \leq \delta_i$  and so FDP-SD begins this analysis at  $i_0$ , the smallest possible index for which  $D_i \leq \delta_i$ . Under Assumption 1, reporting the following list of discoveries  $R_{\alpha, \gamma}$  controls the FDP:

$$R_{\alpha, \gamma} := \{i \in [p] : i \leq k_{FDP}, L_i = 1\}, \quad k_{FDP} := \max\{i : \prod_{j=i_0}^i 1_{D_j \leq \delta_j} = 1 \text{ or } i = 0\}. \quad (3)$$

## 2.1 Extension to side information

In proteomics, so-called *post-processors* such as PeptideProphet [28] and Percolator [26] have popularized the use of side information to increase the number of detected peptides. These tools use machine learning procedures, leveraging features associated with the PSMs, such as the charge state associated with the spectrum and the matched peptide’s length, to better distinguish correct from incorrect PSMs, and hence to deliver more discoveries. These tools have no theoretical guarantees and, having recently pointed out scenarios where such post-processors can fail to control the FDR [18], we will not analyze these tools in this paper.

To our knowledge, the only ‘intrinsic’ competition-based multiple testing procedure that uses arbitrary side information in a data-driven manner is the recent *Adaptive Knockoffs* (AdaKO) by Ren and Candès [44]. AdaKO is a specialization of the p-value based procedure *AdaPT* [33] that we discuss in the next section. By ‘intrinsic’, we mean that while other p-value based approaches may be modified to be used in the competition setting, they are significantly less powerful and do not really qualify in this sense, as demonstrated in [44]. Adaptive Knockoffs works by iteratively pruning  $\mathcal{S}$ , the candidate set of hypotheses, selecting each time the hypothesis it deems most likely to be a true null. To do that, it fits a classification algorithm using a strict set of information that partially masks the data: the scores  $W$ , the side information  $\mathbf{x}$ , and the labels  $L_i$  of the hypotheses that were pruned up to that point ( $i \in [p] \setminus \mathcal{S}$ ), as well as  $\#\{L_i = 1 : i \in \mathcal{S}\}$  and  $\#\{L_i = -1 : i \in \mathcal{S}\}$ . In their paper, Ren and Candès investigate this pruning strategy using different types of ‘filters’: a logistic regression (LR), a generalized additive model (GAM) which is the default filter in their R package, a random forest (RF), and a two-group probabilistic model which is fitted using the expectation-maximization algorithm (EM) [13]. The pruning process terminates when the estimated FDR is less than or equal to  $\alpha$ :

$$\widehat{FDR}_{\mathcal{S}} := \frac{\#\{i \in \mathcal{S}, L_i = -1\} + 1}{\#\{i \in \mathcal{S}, L_i = 1\} \vee 1} \leq \alpha. \quad (4)$$

The remaining positively labeled hypotheses in  $\mathcal{S}$  are then reported. It was shown that, given the following natural extension of Assumption 1, Adaptive Knockoffs controls the FDR.

**Assumption 2.** *Let  $N$  be the indices of the true null hypotheses. The labels  $\{L_i : i \in N\}$  are i.i.d.  $\pm 1$  uniform random variables independent of all the scores  $W$ , the side information  $\mathbf{x}$ , and the labels of the false null hypotheses.*

## 3 Background: p-value based multiple testing

Multiple testing with FDR control was popularized by Benjamini and Hochberg when they developed the first testing procedure of this kind, which we refer to as the ‘BH procedure’ [2]. Since then, many p-value based methods that control the FDR have been developed to improve statistical power.

One such strategy for improving on BH involves estimating the fraction of true null hypotheses, denoted as  $\pi_0$ . Indeed, the BH procedure controls the FDR conservatively at level  $\pi_0 \cdot \alpha$  instead of  $\alpha$ . Hence, in cases when  $\pi_0 \ll 1$ , the BH procedure loses a considerable amount of power. Methods like those by Storey *et al.* [46] and Benjamini *et al.* [3] estimate  $\pi_0$ , and essentially ‘plug-in’ the estimate  $\hat{\pi}_0$ , by applying the BH procedure at a threshold of  $\alpha/\hat{\pi}_0$  instead of  $\alpha$ .

Instead of the FDR, Guo and Romano’s stepdown approach [20], which we refer to as GR-SD, controls the FDP. In fact, this stepdown approach inspired the development of FDP-SD in the competition setting. GR-SD works by first sorting the p-values in ascending order, i.e.,  $p_1 \leq p_2 \leq \dots \leq p_m$ . Then it constructs a sequence of thresholds,  $\delta_i$  for each p-value  $p_i$  and searches for the largest  $k$  such that  $p_1 \leq \delta_1, \dots, p_k \leq \delta_k$  mutually holds, and then reports the corresponding  $k$  smallest p-values. We provide the pseudocode for this method in Algorithm S3.

### 3.1 Extension to side information

Subsequent approaches were developed to take advantage of scenarios with available side information. Roughly speaking, these methods use side information to weight or rescore the hypotheses, placing higher weights or scores on hypotheses that are believed to be false nulls. Such procedures can be either ‘predetermined’, that is, the weighting or scoring is determined before the actual testing procedure takes place, or ‘adaptive’, in which the weighting or scoring is selected according to the data at hand and therefore often leads to greater statistical power.

Method	Error control	Speed
AdaPT (2018)	Finite FDR	Slow
AdaPT <sub>g</sub> (2021)	Finite FDR	Slow
AdaPT-GMM <sub>g</sub> (2021)	Finite FDR	Slow
ZAP-asymp (2022)	Asymptotic FDR	Fast
AdaFDR (2019)	Asymptotic FDP	Fast

Table 1: Summary of some popular and recent p-value based multiple testing procedures that use side information, indicating each method’s type-1 error control and speed.

Such adaptive methods include *Adaptive P-value Thresholding* (AdaPT) and its derivatives [8, 33], *Z-value Adaptive Procedures* (ZAP) [35] and *AdaFDR* [51]. Table 1 provides a qualitative summary of each method in terms of its type-1 error control, its error control guarantees, and its computational speed. Notably, none of these mentioned tools offers a fast finite type-1 error control, and as we will see, some of these methods have variable power when considering a range of simulated and real datasets. We next provide some background on each of those methods.

AdaFDR splits the pairs  $(p_i, \mathbf{x}_i)_{i=1}^m$  into two folds. For each fold, the method fits a mixture model to optimally rescore the hypotheses, and the model is then applied to the other fold where a list of discoveries is obtained. The two list of discoveries are joined together and then reported. AdaFDR’s mixture model is a composition of Gaussian components to model local ‘bumps’ of genuine signals (false nulls) within the data plus an additional component that captures the monotonic relationship between the side information and the signals.

AdaPT iteratively prunes a candidate set of hypotheses  $\mathcal{S}$ , similar to Adaptive Knockoffs, which was derived from it. At each iteration, AdaPT fits a two-group mixture model on a strict set of information: the p-values outside  $\mathcal{S}$ , the *masked* p-values in  $\mathcal{S}$  given by  $\{p_i \wedge (1 - p_i) : i \in \mathcal{S}\}$  where  $1 - p_i$  is referred to as the *mirrored* p-value, the side information  $\mathbf{x}$ , as well as  $\#\{p_i > 1/2 : i \in \mathcal{S}\}$  and  $\#\{p_i < 1/2 : i \in \mathcal{S}\}$ . It then removes the hypothesis from  $\mathcal{S}$  that is deemed most likely to be a true null based on the fitted model. To fit the mixture model, the EM algorithm is used.

The M-step of the EM algorithm results in a regression problem which allows the user to flexibly use the regression method of their choice. The authors considered a generalized additive model (GAM), a generalized linear model (GLM), and a generalized linear model with  $L_1$  regularization (GLMnet). If we identify each p-value  $p_i > 1/2$  with a label  $L_i = -1$  and each p-value  $p_i < 1/2$  with a label  $L_i = 1$ , then AdaPT terminates this pruning procedure when the estimated FDR, as in Equation (4), is  $\leq \alpha$ . The rationale is that for true null hypotheses, the p-values are usually uniformly distributed, so  $\#\{L_i = -1 : i \in \mathcal{S}\}$  estimates the number of true null hypotheses with positive labels,  $\#\{L_i = 1 : i \in \mathcal{S}\}$ . It then reports the remaining positively labeled hypotheses in  $\mathcal{S}$ .<sup>3</sup>

AdaPT<sub>g</sub> generalizes AdaPT by constructing asymmetric regions to define the positive and negative labels. For example, the p-values  $p_i \in (0.3, 0.9)$  can be identified with a label  $L_i = -1$  and the p-values  $p_i < 0.3$  can be identified with a label  $L_i = 1$ . One advantage of defining these asymmetric regions, is to avoid overestimating the number of true null hypotheses in cases where their p-values are not uniformly distributed and there is a concentration of true null p-values near 1. Subsequently, the estimated FDR needs to be adjusted to account for the fact that we expect twice as many true null p-values with negative labels than positive labels. Moreover, the masked p-values are also no longer  $p_i \wedge (1 - p_i)$ , since  $1 - p_i$  no longer ‘correctly mirrors’ the values in  $(0.3, 0.9)$  onto  $(0, 0.3)$  and therefore needs adjustment. In essence, the rest of the procedure remains the same. Lastly, AdaPT-GMM<sub>g</sub> replaces the two group mixture model in AdaPT/AdaPT<sub>g</sub> for a Gaussian mixture model (GMM). Similar to AdaPT/AdaPT<sub>g</sub>, it also allows the user to choose from a collection of regression methods to fit the model at the M-step of the EM algorithm.

Lastly, ZAP-asympt directly fits a beta mixture model to the data but is only able to offer asymptotic FDR control. Importantly, ZAP-asympt can operate directly on the test statistic instead of just the corresponding p-values to rerank the hypotheses. This is particularly advantageous for two-sided tests because the test statistic is mapped to its p-value in a non-bijective manner, losing information regarding the sign of the original test statistic along the way. Note that AdaPT-GMM<sub>g</sub> can also operate on test statistics, but in this paper, we focus on the p-value information.

The list of methods we examine here is incomplete. Others include *Independent Hypothesis Weighting* [24, 25] which splits the p-values and side information into several folds and learns a weight for each hypothesis within that fold using out-of-fold information. This was shown to control the FDR asymptotically, and with some later adjustments to the method, finite sample FDR control was achieved. Another is *Structure Adaptive Benjamini Hochberg Algorithm* (SABHA) [37], which performs a reweighting of the p-values (similar to IHW) with finite sample FDR control. In addition, *ZAP-finite* is the analogue of ZAP-asympt which offers finite-sample FDR control. It uses the same principles of the AdaPT methods where each hypothesis is pruned one at a time. However, in previous simulations and real data experiments, IHW and SABHA appeared to be consistently outperformed by some of the methods in Table 1. Because we consider the same simulations and real data experiments, we did not include those methods in our comparisons. In addition, ZAP-finite is presented as a less powerful alternative to ZAP-asympt with the computational costs of the AdaPT methods. Given our comparisons to ZAP-asympt and the AdaPT methods, we decided to exclude ZAP-finite from our comparisons.

## 4 RESET (REScoring via Estimating and Training)

RESET is designed to control the FDR or the FDP in either the competition or p-value based setting. We next describe RESET’s main steps, with further details given in Algorithm S4. In Section

<sup>3</sup>AdaPT and AdaPT<sub>g</sub> do not use labels explicitly — we introduce those here for notational convenience.

S.3, we prove that RESET controls the FDR/FDP in the finite-sample setting. For simplicity, we use the target-decoy terminology, i.e., we refer to a hypothesis with  $L_i = 1$  as a ‘target win’ or a target for short, and  $L_i = -1$  as a ‘decoy win’ or a decoy for short.

#### 4.1 RESET outline

1. Intrinsically, RESET’s input consists of the labels, winning scores, and side information  $(L, W, \mathbf{x})$ . Hence, in the p-value setting, each  $p_i$  is first converted to a pair  $(L_i, W_i)$  in the following way:

$$L_i = \begin{cases} +1 & p_i \in [0, a) \\ -1 & p_i \in (b_1, b_2] \end{cases}, \quad W_i = \begin{cases} |\Phi^{-1}(p_i)| & p_i \in [0, a) \\ |\Phi^{-1}((b_2 - p_i) \cdot \frac{a}{b_2 - b_1})| & p_i \in (b_1, b_2] \end{cases}, \quad (5)$$

where  $0 < a \leq 1/2 \leq b_1 < b_2 \leq 1$  determine the cutoff regions for defining a positive and negative label, and  $\Phi$  is the standard normal CDF. Hypotheses with p-values outside of  $[0, a) \cup (b_1, b_2]$  are thrown out. The default is  $a = b_1 = 1/2$  and  $b_2 = 1$ .

2. RESET independently and randomly assigns each winning decoy as a *training* decoy with probability  $s$  (we used  $s = 1/2$  throughout). The complementary set of decoy wins defines the *estimating* decoy set, and the set of *pseudo*-targets is the set of all estimating decoys and target wins. The *pseudo* labels,  $\tilde{L}_i$ , denotes whether the  $i$ th hypothesis is a pseudo-target ( $\tilde{L}_i = 1$ ) or a training decoy ( $\tilde{L}_i = -1$ ).
3. Next, RESET applies a user-selected semi-supervised machine learning model which uses the pseudo labels, winning scores, and side information  $(\tilde{L}, W, \mathbf{x})$ . Note that this is a semi-supervised task because the positive pseudo labels typically contain a mixture of true and false nulls, while the negative pseudo labels indicate true null hypotheses.

The output of this step is a rescoring of the training decoys and pseudo-targets, denoted as  $\tilde{W}$ . Ideally,  $\tilde{W}$  scores many of the false nulls among the pseudo-targets higher than they were scored originally. We provide a specific framework that we developed for this crucial step in Section 4.3.

4. With the training complete, the training decoys are thrown out, and the original labels  $L$  of the remaining pseudo-targets are revealed.
5. RESET then determines its list of discoveries by applying to the pseudo-targets using the original labels  $L$  and the new scores  $\tilde{W}$  either
  - SSS+ (Algorithm S1) at the desired level  $\alpha$  for FDR control, or
  - FDP-SD (Algorithm S2) at the desired level  $\alpha$  and confidence parameter  $\gamma$  for FDP control.

The two algorithms, SSS+ and FDP-SD, require an additional parameter  $c$ . This parameter is used to define the expected ratio of the number of null targets to decoys,  $\frac{c}{1-c}$ . Typically, this is set to  $c = 1/2$  for an expected target-decoy ratio of 1; however, RESET uses approximately half of the decoys for training purposes (by default). Since those decoys are subsequently thrown out, this parameter needs to be adjusted. Indeed, assuming that the labels  $L$  of the true nulls are *i.i.d.* uniform  $\pm 1$  RVs, and  $s = 1/2$ , we set the parameter  $c = 2/3$ , so



that the expected target-decoy ratio is 2. More generally, if we know that for a true null  $\mathbb{P}(L_i = 1) \leq c_0$ , then we set  $c = \frac{c_0}{1-s \cdot (1-c_0)}$ . For example in the p-value setting,  $c_0 = \frac{a}{a+b_2-b_1}$ . This choice is made rigorous in Lemma S1.

We note that the above application of  $\Phi^{-1}$  in Equation (5) is not strictly necessary for type-1 error rate control. We apply  $\Phi^{-1}$  to the p-value  $p_i$  or the mirrored p-value  $(b_2 - p_i) \cdot \frac{a}{b_2 - b_1}$  because we found that doing so makes the semi-supervised learning task of Step 3 to be generally less variable and more powerful (data not shown).

Crucially in Step 4, the training decoys are thrown out. This is important since during the training phase of Step 3, the semi-supervised machine learning model will have presumably learned to discriminate between the training decoys and the pseudo-targets. Hence, true null targets will tend to score higher than the training decoys making the latter unsuitable for estimating the number of true nulls among the top scoring hypotheses.

## 4.2 RESET controls the FDR or FDP

To establish RESET’s control of the FDR or FDP in both the competition and p-value settings, we generalize Assumption 2 when the distribution of the true null labels  $\{L_i : i \in N\}$  is non-uniform. This is given below:

**Assumption 3.** *Let  $N$  be the indices of the true null hypotheses. The labels  $\{L_i : i \in N\}$  are *i.i.d.*  $\pm 1$  random variables with  $\mathbb{P}(L_i = 1) \leq c_0$  and are independent of all the scores  $W$ , the side information  $\mathbf{x}$ , and the labels of the false null hypotheses.*

In the p-value setting, Assumption 3 is satisfied under some mild conditions regarding the distribution of the true null p-values. The value of  $c_0$  is determined by the cutoff regions  $[0, a)$  and  $(b_1, b_2]$  which are used to assign the positive or negative labels (Equation (5)). This is given by the following Lemma originally established by Chao and Fithian [8].

**Lemma 1** (Chao and Fithian). *Assume that the true null p-values have a non-decreasing density and that they are mutually independent and that they are independent of the false null p-values as well as of all the side information. Then Assumption 3 is satisfied with  $c_0 = \frac{a}{a+b_2-b_1}$ .*

The above lemma is phrased differently by Chao and Fithian and is presented as Lemma A.1 in their paper, but it is materially the same. Most of the time, we will consider symmetric cutoff regions  $[0, 1/2)$  and  $(1/2, 1]$ . For completeness, we provide a proof of this lemma in Supplementary Section S.2 using our notation.

In practice, Assumption 3 (or the conditions of Lemma 1) needs to be verified. We provide reasonable heuristic justification of this assumption in our real data applications in Sections 5.2 and 6.2. We are now ready to state our two main theorems.

**Theorem 1.** *Under Assumption 3 RESET controls the FDR at the user-specified threshold  $\alpha$ .*

**Theorem 2.** *Under Assumption 3 RESET controls the FDP at the user-specified threshold  $\alpha$  and confidence  $1 - \gamma$ .*

We defer the proof of RESET’s FDR and FDP control to Supplementary Section S.3. The proof requires an intermediate lemma (Lemma S1), which states that the labels  $L$  of the true null pseudo-targets in Step 4 remain *i.i.d.*  $\pm 1$  RVs independently of everything else, even after sampling the training decoys in Step 2 and the application of the machine learning model in Step 3.

### 4.3 Semi-supervised approach

In this section we describe our specific framework for RESET’s Step 3, which as mentioned, can use any semi-supervised machine learning model. It consists of two main steps: (1) we apply a range of classification algorithms to estimate a high quality positive set from the data, containing presumably many false nulls, and (2) this positive set is then subsequently used for a second application of the classification algorithms to rescore the hypotheses.

- i. Define the negative set as the set of all training decoys and the positive set as a subset of the top scoring pseudo-targets (which we elaborate on in Step III at the end of this section). We define the features that are subsequently used by a collection of classification algorithms as the combined score and side information  $(W, \mathbf{x})$ .
- ii. For each considered classification algorithm, we randomly split all the hypotheses into  $K$  folds (we used  $K = 3$  throughout). For each  $k \in \{1, 2, \dots, K\}$ , we train the classification algorithm using the positive and negative set on the features in the  $K \setminus \{k\}$  folds and apply the trained model to all the hypotheses in the  $k$ th test fold. We consider a random forest (RF), a generalized additive model (GAM), and a collection of two-layer neural networks (NN) with decay parameter  $\lambda \in \{0, 0.1, 1\}$  and a number of hidden layer nodes  $h \in \{2, 5, 10\}$ .
- iii. To reduce variability, we repeat Step ii  $r$  times (we used  $r = 10$ ).
- iv. To evaluate each classification algorithm, we apply Selective SeqStep (SSS) (Algorithm S1, which is similar to SSS+ of Equation (2) without the ‘+1’) at an FDR threshold  $\alpha$  to each of the  $rK$  test folds, using the scores obtained from the classification algorithm and the pseudo labels. If  $\mathbb{P}(L_i = 1) \leq c_0$  then we set  $c = 1 - s \cdot (1 - c_0)$ . This is to ensure that the ratio  $\frac{c}{1-c}$  correctly accounts for the number of null pseudo-targets to training decoys<sup>4</sup>.
- v. We record the total number of ‘discoveries’ produced by SSS over the  $rK$  test folds from the previous step and select the classification algorithm that maximizes this value.
- vi. Using the chosen classification algorithm, we assign new scores  $\tilde{W}$  to the hypotheses.  $\tilde{W}_i$  is defined as the average decision value for the  $i$ th hypothesis in the test fold that it appears in, taken over the  $r$  repetitions executed in Step iii.
- vii. We reapply Selective SeqStep (SSS) at  $\alpha$  using the pseudo labels and the updated scores,  $(\tilde{L}, \tilde{W})$  with  $c = 1 - s \cdot (1 - c_0)$ .
- viii. The positive set is redefined as those pseudo-targets that are ‘discovered’ in Step vii. Steps ii-vi are then repeated with the new positive set. To ensure that the positive set is not too small, we increase  $\alpha$  by increments of 0.01 until the positive set reaches `min_positive` or until all the pseudo-targets are in the positive set. We used `min_positive = 50`.
- ix. The final scores  $\tilde{W}$  are then reported.

We apply the following additional heuristics to our implementation that occur prior to Step 1 and leave some minor details in Section S.4.

- I. RESET throws out the hypotheses with undefined labels, i.e., those hypotheses with  $W_i = 0$ . This effect is negligible when using p-values. However, in variable selection, the LCD score

---

<sup>4</sup>This is not a requirement for error control.

in the knockoff filter forces many of the winning scores to be zero ( $W_i = 0$ ), leaving typically a few hypotheses to be considered by RESET and consequently losing some information. We try to recover some of this information in the following way. For each hypothesis with  $W_i \neq 0$ , we identify the  $k$ -nearest neighbors in terms of the side information (zero-scoring hypotheses included). Then we define an extra side information variable as the number of zero-scoring hypotheses among these identified neighbors (we used the 20-nearest neighbors).

- II. To reduce the effect of ‘noisy’ side information that is unable to distinguish between true and false nulls, we implement an initial side information selection procedure. That is, we use a generalized additive model to fit a smoothing spline using  $W \cdot \tilde{L}$  as the response against each user-provided side information variable one at a time. We use `tryCatch` in case the smoothing spline fails, in which case we fit the response directly to the side information variable, that is, we use a linear fit. Again, we try to make use of some of the zero-scoring hypotheses setting  $W \cdot \tilde{L} = 0$  in these cases. We keep only the side information variables with sufficiently small  $p$ -values in the fitted model ( $p < 0.01$ ).
- III. Not all the pseudo-targets need to be included in the initial positive set in Step i. After all, we expect many of the pseudo-targets to be true nulls. Hence, to improve the performance of RESET, we consider the following strategy. For each feature in  $(W, \mathbf{x})$ , reorder the hypotheses according to that feature, and apply SSS to the pseudo labels  $\tilde{L}$  at the FDR level  $\alpha$ . Then select the feature that maximizes the number of pseudo discoveries. Then using the chosen feature, we define the positive set as those pseudo-targets discovered at  $\alpha_0$ , again using SSS with the pseudo labels  $\tilde{L}$  (we used  $\alpha_0 = 50\%$  throughout). Usually the score is selected, but in some cases the side information is highly informative and is selected instead.

Users interested in a small FDR level, like  $\alpha = 1\%$ , could probably benefit from reducing  $\alpha_0$  to further improve the performance, and in particular the speed, of RESET (though as we mentioned, we kept  $\alpha_0 = 50\%$  across the board). To ensure that the positive set is not too small, we increase  $\alpha_0$  by increments of 0.01 until the positive set reaches `min_positive` or until all the pseudo-targets are in the positive set.

We refer to the general RESET wrapper in combination with the above semi-supervised approach as *RESET Ensemble*. We refer to *RESET RF/GAM/NN* when the ensemble of machine learning methods in Step ii is reduced to a random forest, generalized additive model, and a collection of neural networks as described, respectively.

#### 4.4 Code availability

Our code is available at [https://github.com/freejstone/stat\\_RESET\\_paper\\_code](https://github.com/freejstone/stat_RESET_paper_code) with an Apache-2.0 license. We intend to develop a package for RESET in R.

## 5 Experiments: competition setting

### 5.1 Numerical experiments

In this section, we conduct a wide range of simulations in the variable selection problem based on those introduced by Ren and Candès [44]. We compare RESET Ensemble to Adaptive Knockoffs (AdaKO) and the generic Knockoff Filter (KO) (see Section 2). Further implementation details for AdaKO are given in Supplementary Section S.5. We provide a brief description of each simulation setup, referring to [44] for further details. Each setup is designed to satisfy Assumption 3,

which is required for our theoretical guarantees. The labels and scores are obtained according to Equation (1). We focus on FDR control in this section, and we study FDP control in Section 5.2.

### 5.1.1 Simulation 1: Linear model with one-dimensional side information

Our first simulation is based on Simulation 1 by Ren and Candès [44]. They used  $n = 1000$  independent observations from the joint data distribution of  $(X, Y)$ , where  $X$  is drawn from a hidden markov model (HMM) with  $p = 900$  variables and  $Y|X \sim \mathcal{N}(X\beta, 1)$  is a linear model. The  $\beta$ 's are selected in the following way. Let  $k$  denote the number of nonzero  $\beta$ 's. Then  $k$  indices from  $\{1, 2, \dots, p\}$  are sampled without replacement with indices  $i \in \{1, \dots, 2k\}$  having probability proportional to  $1/i^2$  and the indices  $i \in \{2k + 1, \dots, p\}$  having zero probability. The  $k$  chosen indices are the nonzero  $\beta$ 's and are assigned a value of  $\pm 3.5/\sqrt{n}$  where the signs are chosen *i.i.d.* uniformly. We consider  $k \in \{50, 150, 300\}$  while the original simulation only considers  $k = 150$ . Each hypothesis is supported by the side information  $\mathbf{x}_i = i$ , which should help in detecting the nonzero  $\beta$ 's, because smaller values of  $i$  are more likely to correspond to a nonzero  $\beta_i$ . We used 100 independent runs of the above, where each run consisted of drawing those  $n$  observations. The original simulation in [44] sampled the  $\beta$ 's once and fixed them across the 100 runs. Here we redrew the  $\beta$ 's for each run so that we may average our results over a range of models, as we noticed that all the methods exhibited significant variability between the draws.

### 5.1.2 Simulation 2: Linear model with two-dimensional side information

In a second simulation, we considered a larger linear model where  $n = 2000$  observations are taken from the joint distribution  $(X, Y)$  as described in Section 5.1.1, with  $p = 1800$ . Accordingly, we also adjusted the number of false nulls to  $k \in \{150, 300, 450\}$ . Note that unlike the previous simulation, it is not relevant how the  $k$  variable indices are selected from  $\{1, 2, \dots, p\}$ . Each hypothesis is equipped with the following two-dimensional side information. For the  $i$ th hypothesis, we draw a pair of observations  $\mathbf{x}_i$  from a bivariate normal  $\mathcal{N}(\boldsymbol{\mu}, I)$  with  $\boldsymbol{\mu} = (0, 0)$  for a true null hypothesis and  $\boldsymbol{\mu} = \pm(2, 2)$  for a false null hypothesis, where the signs are chosen *i.i.d.* uniformly. We used 20 independent runs of this larger simulation instead of 100, where in each run we draw those  $n$  observations,  $\beta$  coefficients, and side information variables.

### 5.1.3 Simulation 3: Logistic model with two-dimensional side information

Next, we consider Simulation 2 by Ren and Candès [44]. They generate  $n = 1000$  observations with  $p = 1600$  variables sampled from the joint data distribution of  $(X, Y)$ , where  $X$  is distributed according to a multivariate normal distribution and  $Y|X \sim \text{Bernoulli}(e^{\beta \cdot X} / (1 + e^{\beta \cdot X}))$  is a logistic model (see [44] for further details). Each hypothesis' side information is a unique pair of values  $\mathbf{x}_i = (\mathbf{x}_{i1}, \mathbf{x}_{i2})$  from the lattice  $[-20, 19] \times [-20, 19] \subseteq \mathbb{Z}^2$ . The nonzero  $\beta$ 's are chosen according to the position of  $(\mathbf{x}_{i1}, \mathbf{x}_{i2})$  in the lattice. An image of the nonzero  $\beta$ 's is given in Figure 1. Each nonzero  $\beta$  is set to  $\pm 25/\sqrt{n}$  where the signs are chosen *i.i.d.* uniformly. We used 98 runs of the above setup (since in 2 runs, AdaKO EM failed with an error), where each run consisted of drawing those  $n$  observations. The original simulation in [44] sampled the sign of the  $\beta$ 's once, fixing them across the 100 runs. Instead, we redraw the sign of the  $\beta$ 's in each of the 98 runs since we found that the results of all the methods significantly varied with those draws.

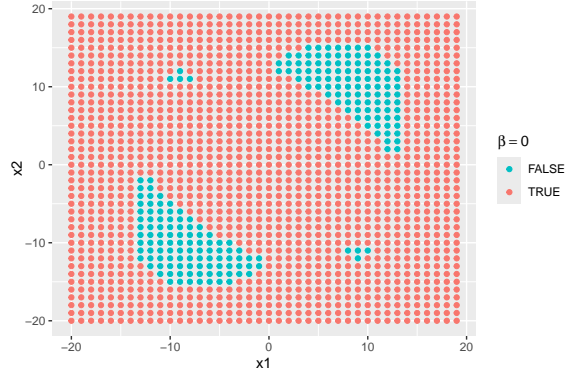


Figure 1: **Location of nonzero  $\beta$ 's according to the pair of values  $(x, y)$  in the lattice.** The same image is given in [44].

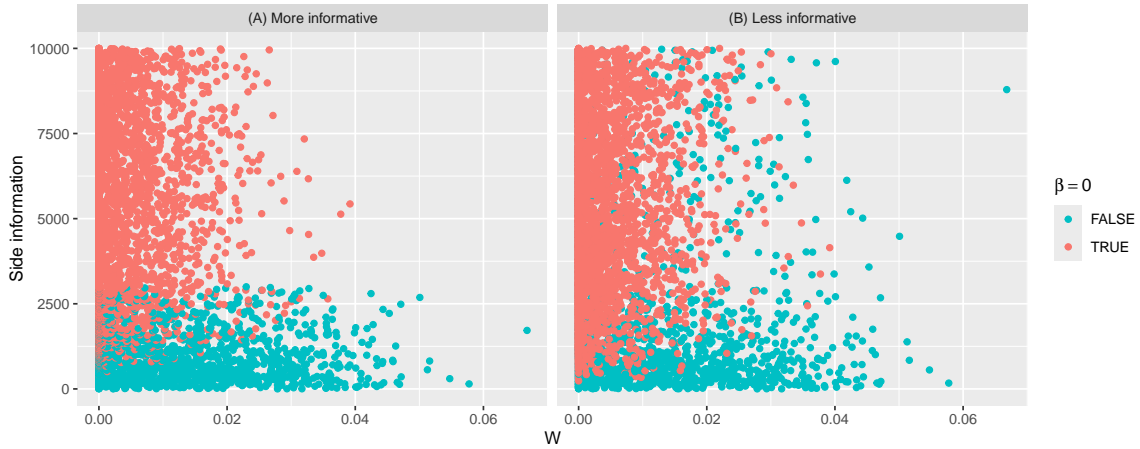


Figure 2: **Scatterplot of each hypothesis according to the LCD score denoted as  $W$  (x-axis) and side information variable (y-axis).** Each hypothesis is colored according to whether it is a true (red) or false null hypothesis (blue). In (A), the side information variable is the index of the hypothesis in Simulation 1 (Section 5.1.1). In (B), we use one of the three side information variables as described in Simulation 4 (Section 5.1.4).

#### 5.1.4 Simulation 4: Large $p$ and $n$ and 3-d side information

Finally, in the last simulation,  $n = 10K$  observations with  $p = 10K$  variables and  $k = 0.15p$  relevant variables are drawn from the joint data distribution  $(X, Y)$  exactly as described in Simulation 1. Each variable is equipped with the following three-dimensional side information. The first  $k$  variables are randomly assigned a value drawn from  $i \in \{1, \dots, 2k\}$  taken without replacement and having probability proportional to  $1/i^2$ . The remaining  $p - k$  variables are uniquely assigned to one of the remaining values from  $\{1, 2, \dots, p\}$  uniformly at random. We expect most of the nonzero  $\beta$ 's to have small values of  $i$ , but the effect of the random assignment makes the resulting side information variable less informative than in Simulation 1, as depicted in Figure 2. This process is repeated three times, thus associating three side information variables with each hypothesis, which taken together, should be reasonably informative. We conducted 5 independent runs, where in each run we drew the  $n$  observations,  $\beta$  coefficients, and side information.

### 5.1.5 Results

We first compare RESET Ensemble with Adaptive Knockoff’s default method in R, AdaKO GAM, and the generic Knockoff Filter (KO). In Figure 3, for each simulation we plot the power of each method as a function of the selected FDR thresholds of  $\alpha \in \{0.05, 0.1, 0.2, 0.3\}$ . The power is calculated as the proportion of relevant variables correctly discovered, averaged over the number of runs used in each simulation. Similarly, in Supplementary Figure S2, we plot the estimated FDR: the proportion of irrelevant variables in the discovery list, averaged over the runs.

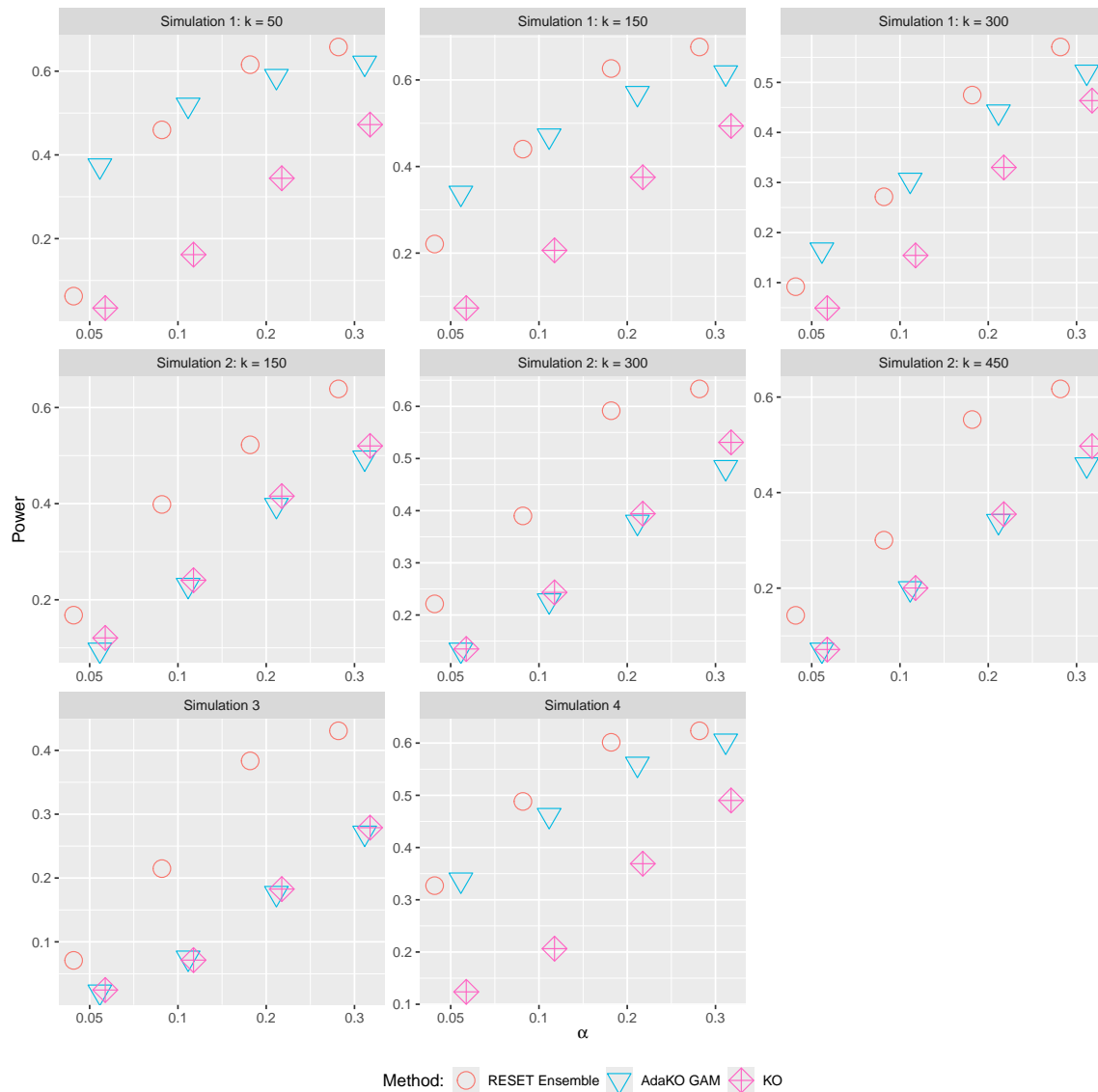


Figure 3: **RESET Ensemble vs. AdaKO GAM vs. KO**. Each panel plots the power for each method at FDR thresholds ranging from 5% to 30%. The first row corresponds to Simulation 1 with three values of  $k \in \{50, 150, 300\}$ , the second row corresponds to Simulation 2 with three values of  $k \in \{150, 300, 450\}$ , and the last row corresponds to Simulation 3 and 4. For readability, the points are jittered in the horizontal direction. A description of AdaKO GAM and KO can be found in Section 2.

Unsurprisingly, RESET Ensemble uniformly dominates KO, demonstrating that it successfully leverages the side information. At the same time, AdaKO GAM mostly improves on KO, with some exceptions.

In Simulation 1, we find that at higher FDR thresholds, RESET Ensemble is the preferred approach in terms of power. On the other hand, AdaKO GAM is more powerful than RESET at lower FDR thresholds, particularly in the case of  $k = 50$  and  $\alpha = 5\%$ . This is not too surprising for two reasons. First, RESET trains its classification algorithms on a relatively small positive set of false nulls. Second, RESET incurs a greater cost in terms of power at lower FDR thresholds if the classification algorithm overfits and incorrectly scores a knockoff higher than it should. Indeed, at an FDR threshold of  $\alpha = 5\%$ , each knockoff may cost up to  $2/\alpha = 40$  discoveries.

We find in Simulations 2 and 3 that RESET Ensemble is consistently more powerful than AdaKO GAM; in fact, AdaKO GAM appears to essentially have the same power as KO. The result in Simulation 3 is consistent with the findings of Ren and Candès in their analogous simulation. Indeed, AdaKO GAM does not implement any smooth terms when the number of side information variables is two or more, and is therefore unable to leverage the side information if the true and false null hypotheses are not ‘easily’ separable. Finally in Simulation 4, we see that RESET Ensemble is generally the most powerful, with essentially the same power as AdaKO GAM at  $\alpha = 5\%$ . We hypothesize that the greater number of variables in this example, particularly relevant variables, appears to overcome the relatively poor performance of RESET Ensemble in Simulation 1 at low FDR thresholds.

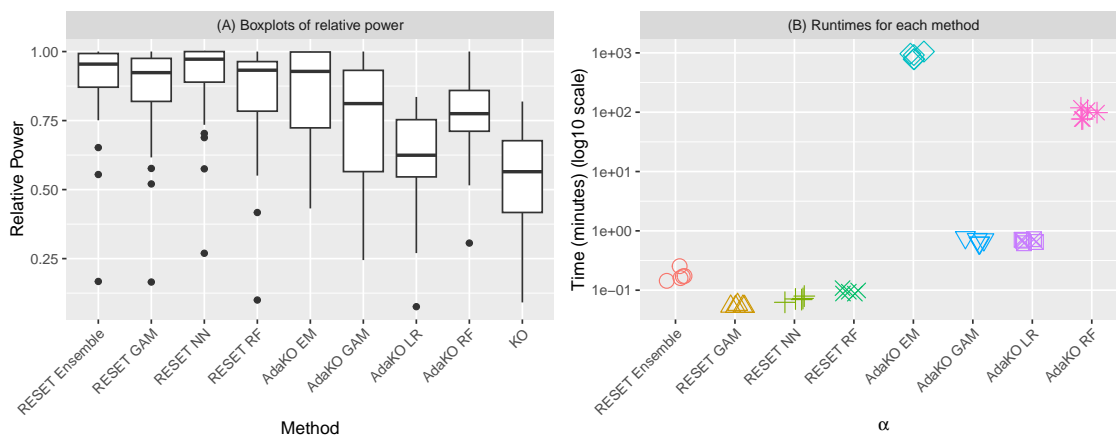


Figure 4: **Relative power and runtimes for each method.** (A) Each boxplot describes the relative powers for each method, computed across the combination of simulations and FDR thresholds in Figure 3. (B) The log10 runtimes of each method applied at the 5% FDR level for 5 runs of Simulation 4. For readability, the points are jittered in the horizontal direction.

We compared RESET Ensemble with AdaKO GAM because those are the respective default methods. We complement this comparison with Figure 4A where we summarize the performance of all RESET and Adaptive Knockoff methods. Specifically, for each panel and FDR threshold in Figure 3, we determined the maximum power across all methods and computed the relative power of each method to this maximum. The resulting relative powers are reported as boxplots, giving an indication of the performance of each method across the simulations as a whole. A plot of the actual powers for each of the methods is given in Supplementary Figure S3. While in Supplementary Figure S3 we often find a version of AdaKO that is more powerful, or at least comparable to RESET Ensemble, this varies between the versions. On the other hand, RESET Ensemble’s performance is consistent across these simulations, and overall typically achieves the highest relative power when the results are aggregated. Interestingly, RESET NN seems to be marginally more powerful than RESET Ensemble. While this may be the case, we still recommend RESET Ensemble as the default

approach to alleviate the burden of selecting any single classification algorithm.

One advantage of RESET is its computational speed. Indeed, our implementation of RESET, as described in Section 4.3, has many steps that can be parallelized: the  $r$  evaluations of each classification algorithm on the  $K$  folds can all be done in parallel using multiple cores. In contrast, Adaptive Knockoffs must iteratively apply a classification algorithm for every nonzero scoring hypothesis in the candidate set  $\mathcal{S}$  until the estimated FDR is  $\leq \alpha$ , or all hypotheses are revealed. Figure 4B demonstrates this advantage showing the ( $\log_{10}$ ) runtimes of RESET (using 10 of a 20-cores CPU) and of Adaptive Knockoffs at the 5% FDR level across 5 runs of Simulation 4. We find that each version of RESET is significantly faster than each version of Adaptive Knockoffs. RESET Ensemble is around  $10^3$  to  $10^4$  times faster than AdaKO EM,  $10^2$  to  $10^3$  times faster than AdaKO RF, and about 3-4 times faster than AdaKO LR and AdaKO GAM. In scenarios, as in Simulations 3 and 4, where AdaKO EM and AdaKO RF are infeasible, and AdaKO GAM and AdaKO LR are unable to leverage the side information RESET is clearly more suitable. We investigate such a commonly encountered scenario in the following application.

## 5.2 Application to peptide detection

In this section we compare RESET to Adaptive Knockoffs in the peptide detection context using mass spectrometry data and show that (a) the Adaptive Knockoff methods are often computationally infeasible, (b) feasibility aside, RESET is more powerful than Adaptive Knockoff’s default filter, AdaKO GAM, when controlling the FDR, and (c) when controlling the FDP, RESET is able to typically discover more peptides than the vanilla FDP-SD. We provide a heuristic justification of Assumption 3, which is required for RESET’s theoretical guarantees, in Section S.15.

### 5.2.1 HEK293 data

We show that the application of Adaptive Knockoffs is often too slow to be used effectively in scenarios such as the peptide detection problem that involve a large amount of data. We demonstrate this using HEK293 data [9], a popular dataset used in benchmarking the development of new software [30, 32, 50] that we downloaded from the Proteomics Identification Database (PRIDE) [41]. After data preparation and searching the combined 24 HEK293 spectrum files, we determined the scores  $Z_i$  for each target peptide and  $\tilde{Z}_i$  for each decoy peptide using the XCorr score function (see Supplementary Section S.12 for details). Next, we competed each pair by recording the score  $W_i = Z_i \vee \tilde{Z}_i$  and label  $L_i = 1$  if  $Z_i > \tilde{Z}_i$  and  $L_i = -1$  if  $Z_i < \tilde{Z}_i$  (ties were randomly broken). In addition to its primary score we associate with each peptide-spectrum match (PSM) a set of features, such as the charge state or peptide length. Each winning peptide inherits these features, or side information  $\mathbf{x}_i$ , from its maximally associated PSM, allowing us to define the desired triples  $(L, W, \mathbf{x})$ . A complete description of the side information used is given in Table S4 of the Supplement.

Finally, using the method described in Supplementary Section S.13, we estimated the time it would take for each method of Adaptive Knockoffs to report discoveries at the 1% FDR level (which is the typical FDR threshold in the peptide detection context). Table 2 shows the average estimated times taken over 5 distinct target-decoy databases, with decoys varying each time by randomly shuffling the target peptides. It is clear that running any implementation of AdaKO is generally too expensive, with the worst being AdaKO RF at an estimate of 836 days, and the default method, AdaKO GAM, taking an estimate of 1.06 days. In contrast, we were able to successfully run RESET Ensemble with FDR control in 27.5 minutes.



Method	Time
RESET Ensemble	27.5 minutes
AdaKO GAM	1.06 days
AdaKO EM	33.71 days
AdaKO LR	3.35 days
AdaKO RF	836.03 days

Table 2: **The average runtimes for each method at 1% FDR on the HEK293 dataset.** The average runtimes reported for each Adaptive Knockoffs method is estimated (as described in Section S.13), while we computed the actual average runtime for RESET Ensemble. The average is taken over 5 randomly constructed decoy databases. We used 20 cores for RESET Ensemble.

## 5.2.2 PRIDE data

Due to the aforementioned runtime problem, we had to use small datasets when evaluating the power of Adaptive Knockoffs in the peptide detection context. Specifically, we focused on thirteen spectrum files (each with  $< 33\text{K}$  PSMs) from the twenty PRIDE-20 datasets that we recently used in [18]. In the following results, we only considered searching the spectrum files once against a single target-decoy database, since unlike RESET we can only feasibly apply a single application of Adaptive Knockoffs. Data preparation, search settings and the detailed definition of the triples  $(L, W, \mathbf{x})$  are given in Supplementary Section S.14 along with the list of side information used in Supplementary Table S5.<sup>5</sup>

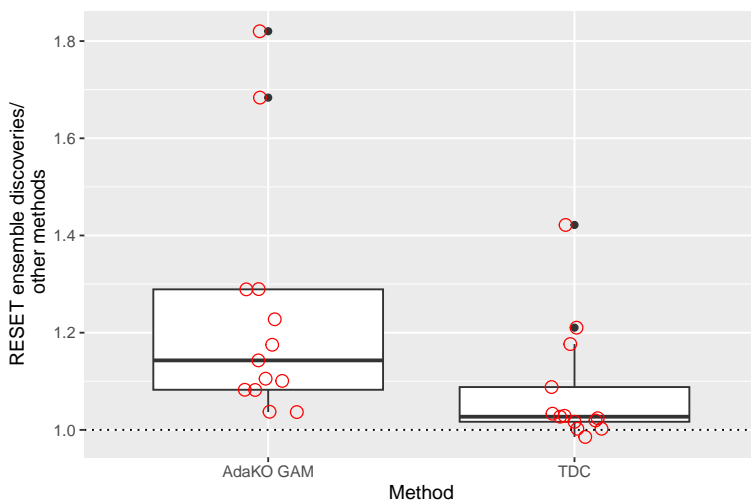


Figure 5: **Comparison of RESET Ensemble and AdaKO GAM.** For each of the 13 PRIDE datasets, we computed the average number of discoveries using 10 applications of RESET Ensemble, varying RESET’s internal seed. The figure shows a boxplot of those RESET Ensemble averages divided by the number of discoveries using AdaKO GAM (left boxplot) and TDC (right boxplot) using the 13 PRIDE-20 datasets (there are total of 13 points for each boxplot).

Figure 5 shows the average number of discoveries reported using 10 applications of RESET Ensemble, each applied at 1% FDR to the same dataset, divided by the number of discoveries reported by AdaKO GAM (left boxplot) and TDC (right boxplot). In each of the 10 applications of RESET, we varied the internal seed which randomly splits the decoys into their training and estimating sets. Clearly, RESET Ensemble is overall more powerful than AdaKO GAM and TDC. Interestingly, the relative ratios of the number of discoveries between AdaKO GAM and TDC

<sup>5</sup>The side information here slightly differs from above due to different search settings.

suggest that AdaKO GAM is reporting *fewer* discoveries than the generic TDC.

In a second comparison, we looked at the performance of RESET Ensemble versus AdaKO RF because in this setup it was the most powerful implementation of Adaptive Knockoffs. In Figure 6A, the left boxplot displays the average number of discoveries by RESET Ensemble, divided by the number of discoveries by AdaKO RF. In six of the thirteen PRIDE spectrum files, we found RESET Ensemble to be the superior method, while in the remaining seven spectrum files, AdaKO RF produced more discoveries. In one dataset, AdaKO RF discovered 1217 peptides while RESET Ensemble only discovered 1104 peptides, about a 10% increase over RESET Ensemble.

We also assessed the computational times of AdaKO RF in Figure 6B, using both the actual and estimated runtimes as outlined in Section S.13. Reassuringly, our estimated times were less than the actual times taken by each method to complete, thus validating the conservative nature of our estimated times in the previous section. Although we find that, when analyzing these smaller spectrum sets, AdaKO RF is the most powerful method of Adaptive Knockoffs, and is competitive to RESET Ensemble power-wise, it is again clear that AdaKO RF is generally too slow with some runtimes exceeding multiple days even for these small datasets. In fact, on the dataset where AdaKO RF outperforms RESET Ensemble by about 10%, it takes 3.07 days for AdaKO RF to discover its peptides while RESET Ensemble takes about half a minute to complete. Figure 6C shows that in the worst case, RESET takes roughly 1 minute. The issue of runtimes is especially problematic considering the fact that multiple spectrum files are often analyzed jointly, as in our HEK293 analysis in the previous section.

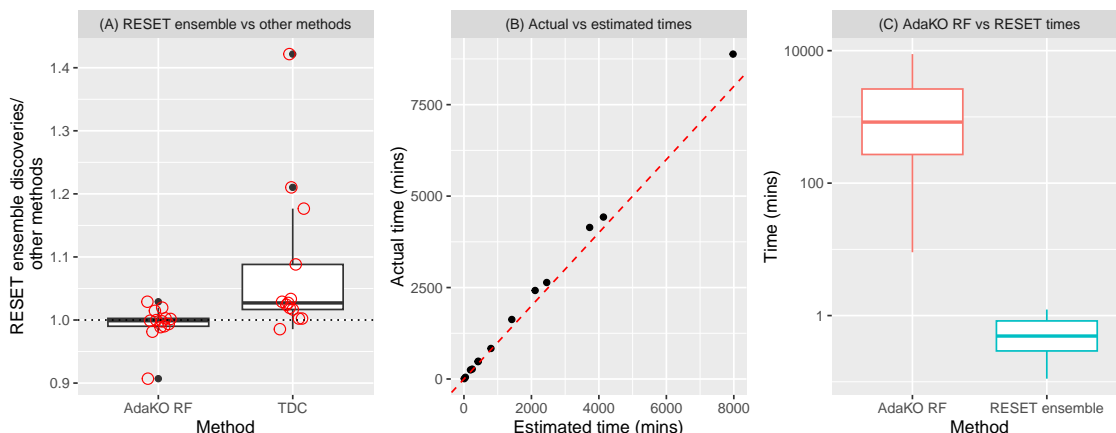


Figure 6: **Comparison of RESET Ensemble and AdaKO RF.** For each of the 13 PRIDE datasets, we computed the average number of discoveries using 10 applications of RESET Ensemble, varying RESET’s internal seed. The left panel shows a boxplot of those average RESET Ensemble discoveries divided by the number of discoveries using AdaKO RF (left boxplot) and TDC (right boxplot) using the 13 PRIDE-20 datasets (there are total of 13 points for each boxplot). In the centre panel, we compare the estimated and actual runtimes for AdaKO RF. Lastly, in the right panel, we compare the actual runtimes of RESET Ensemble and AdaKO RF (in log10 scale).

### 5.2.3 FDP control

Lastly, we evaluated RESET Ensemble’s FDP control using the HEK293 and all twenty PRIDE-20 spectrum files from the previous sections. As in Section 5.2.1, the joint HEK293 spectrum files were searched against 5 distinct target-decoy databases, where each target-decoy database was generated by concatenating the target database to a decoy database consisting of shuffled target peptides. Similarly, each PRIDE-20 spectrum file was searched against 10 distinct target-decoy databases.

We used the `coinflip` version of FDP-SD [40], which provides a uniform increase in the number of discoveries (at the cost of some randomness in the discovery list, see Supplementary Algorithm S2). Our results using RESET Ensemble and FDP-SD are given in Table 3 and Figure 7.

Method	Confidence $1 - \gamma$		
	0.5	0.8	0.9
RESET Ensemble	82987	82729	82558
FDP-SD	75977	75464	75254

Table 3: **The average number of discoveries at 1% FDP threshold at varying confidence parameters using the HEK293 data.** The average number of discoveries reported for RESET Ensemble and FDP-SD on the combined HEK293 spectrum files at different confidence values  $1 - \gamma = 0.5, 0.8, 0.9$ . The averages are taken over 5 applications of each method, once for each of the 5 combined target-decoy databases.

Analyzing the HEK293 results first, RESET Ensemble is clearly more powerful, with an approximately 9–10% increase in the average number of discoveries over FDP-SD at all confidence levels. Analyzing the PRIDE-20 datasets, while RESET Ensemble appears to be generally more powerful, in a few datasets it fails to make any discoveries at high confidence levels. Upon a closer look, the numbers of discoveries made by FDP-SD in these datasets are relatively small, with the largest average number of discoveries among these datasets being 417. When the number of discoveries is expected to be small and the confidence parameter is high, RESET may yield less power, even if the side information is reasonably informative — a phenomenon we dwell on in the Discussion. Regardless, more often than not RESET Ensemble produces more discoveries, and if multiple spectrum files are analyzed jointly, as we do with the HEK293 spectrum files, then the risk of having too few discoveries is reduced.

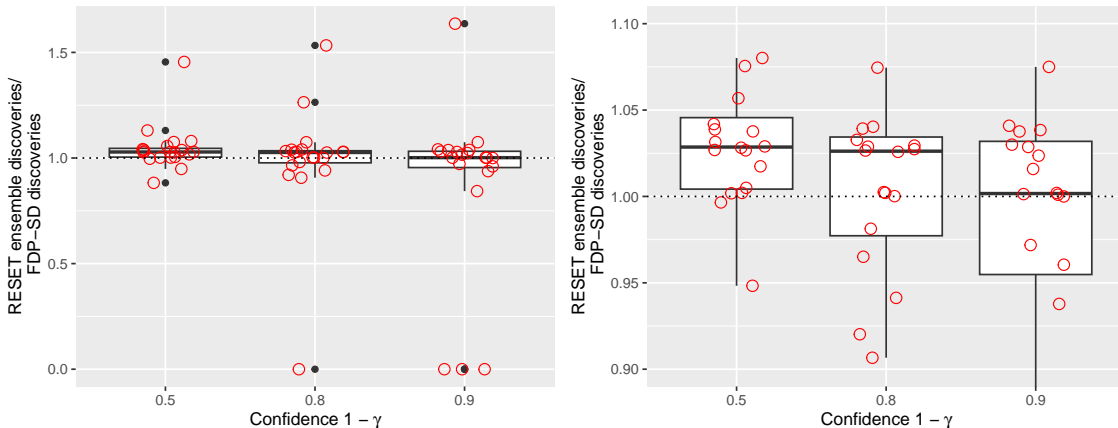


Figure 7: **Comparison of RESET Ensemble and FDP-SD.** The left panel shows boxplots of the average number of discoveries using RESET divided by the average number of discoveries using FDP-SD for each of the twenty PRIDE-20 datasets at a 1% FDP threshold and varying confidence parameters. The averages are taken over 10 applications, one for each of the 10 target-decoy databases used for each PRIDE-20 dataset. The right panel is a ‘zoomed’ in version of the left panel.

The results above consider a canonical ‘narrow’ search. Specifically, during the searching phase, each database peptide and spectrum are only allowed to match if the mass of the database peptide and the observed mass of the sample peptide generating the spectrum, the ‘spectrum mass’, differ by a small amount. Recently, ‘open’ searching, where each spectrum and peptide can match even if their masses differ by hundreds of Daltons, has become a popular method for detecting peptides [30]. Such a search allows for the detection of peptides whose masses have been altered by

*post-translational modifications* (PTMs). We provide further detail in Supplementary Section S.14. In this setting, side information variables such as `dm`, which records the mass difference between the peptide and the spectrum, can be highly informative given that some differences will correspond to masses of common PTMs. Thus, it is not surprising that RESET, which can take advantage of such side information, improves on FDP-SD even further across all confidence levels in this context (Figure 8).

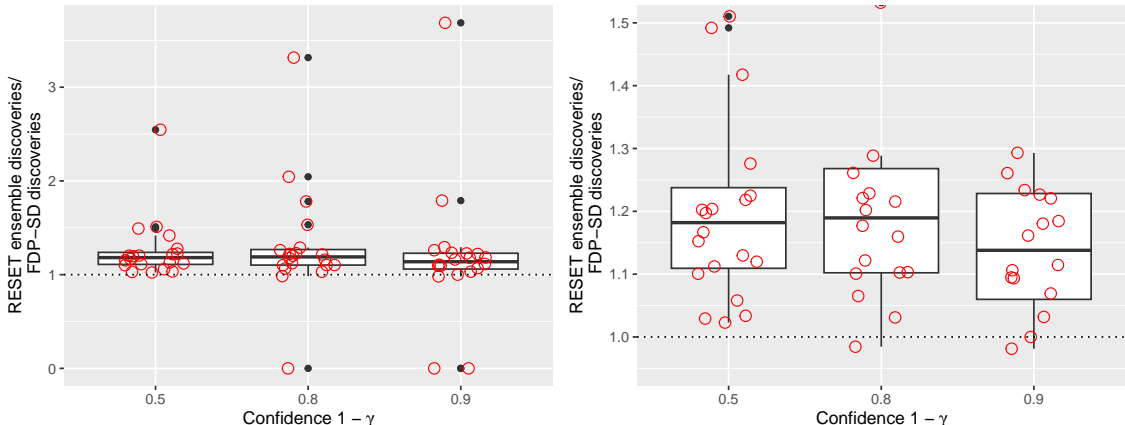


Figure 8: **Comparison of RESET ensemble and FDP-SD using the recently popular ‘open’ search.** The left panel shows boxplots of the average number of discoveries using RESET divided by the average number of discoveries using FDP-SD for each of the PRIDE-20 datasets at a 1% FDP threshold and varying confidence parameters. We implement an ‘open’ search for each PRIDE-20 dataset (see Section S.14). The averages are taken over 10 applications, one for each of the 10 target-decoy databases used for each PRIDE-20 dataset. The right panel is a ‘zoomed’ in version of the left panel.

## 6 Experiments: p-value setting

### 6.1 Numerical experiments

In this section, we consider the p-value setting, comparing RESET with the FDR controlling procedures we reviewed in Section 3.1 on a set of simulations introduced by Lei and Fithian [33]. As in the competition setting, each setup is designed to satisfy Assumption 3, which is required for our theoretical guarantees. Details of each method used are given in Supplementary Sections S.6–S.10.

#### 6.1.1 Simulation 5: p-value based testing with geometric side information

In this section, we look at Simulation 1 of Lei and Fithian [33]. For each hypothesis, they obtain a p-value  $p_i$  from a one-sided normal test so that  $p_i = 1 - \Phi(z_i)$  where  $z_i \sim \mathcal{N}(\mu, 1)$  with  $\mu = 2$  for a false null hypothesis and  $\mu = 0$  for a true null hypothesis. A total of  $m = 2500$  hypotheses are used. Similar to Simulation 3 of Section 5.1.3, each hypothesis’ side information is defined as a unique pair of values  $\mathbf{x}_i = (\mathbf{x}_{i1}, \mathbf{x}_{i2})$  from  $50 \times 50$  equally spaced values in the square  $[-100, 100] \times [-100, 100]$ . The false null hypotheses correspond to certain regions in the square. They considered three scenarios: (a) when the false nulls form a circle in the middle of the square, (b) when the false nulls form a circle in the top right of the square and (c) when the false nulls form an ellipse (Figure 9). We used 100 independent runs, where in each run we randomly draw the 2500 p-values as described.

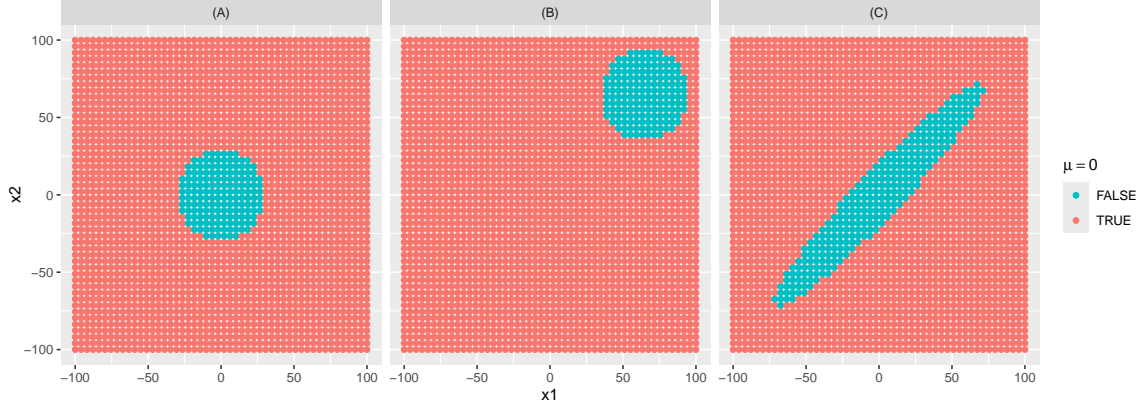


Figure 9: **Location of false null hypotheses according to the pair of values  $(\mathbf{x}_{i1}, \mathbf{x}_{i2})$  in the square  $[-100, 100] \times [-100, 100]$ .** The same picture is given in [33].

Figure 10 shows the results of RESET compared with several p-value based methods that we reviewed in Section 3.1. We find that in the first two simulations, (a) and (b), RESET Ensemble is roughly equal to the best method in terms of power at the 5%, 10% and 20% FDR levels, along with AdaPT/AdaPT<sub>g</sub> GAM. However, in (c), clearly AdaPT/AdaPT<sub>g</sub> GAM are more powerful than the RESET methods, with RESET Ensemble coming arguably as third in the power ranking at the 5%, 10%, and 20% FDR levels. At 1% FDR, all RESET methods have negligible power, although this is consistent with many of the other methods. Interestingly, many of the finite-FDR controlling procedures such as the various RESET and AdaPT methods generally have better power than the asymptotic approaches, ZAP and AdaFDR, suggesting perhaps a misspecification of the fitted model used by these approaches. Figure 10 also shows the estimated FDR of each method. We find that in (a), AdaFDR’s estimated FDR at 20% (21.2% estimated FDR with 50% power) slightly exceeds the FDR threshold. This is possibly explained by the fact that AdaFDR only guarantees asymptotic FDP control. Consistently, Chao and Fithian [8] reported inflated estimated FDRs at high thresholds in simulation studies for AdaFDR.

### 6.1.2 Simulation 6: p-value based testing with 100-dimensional side information

In Simulation 2 of Lei and Fithian [33], the side information for  $m = 2000$  hypotheses consists of 100 *i.i.d.* draws from  $U[0, 1]$ . This setup simulates ‘noisy’ side information since only the first 2 of the 100 draws are used in distinguishing between the true and false null hypotheses. Each p-value  $p_i$  is drawn *i.i.d.* from a two-group beta mixture model, where the true nulls have a uniform distribution and the false nulls have an alternative beta distribution. Specifically, the beta mixture model is given by:

$$f(p_i | \mathbf{x}_i) = 1 - \pi(\mathbf{x}_i) + \pi(\mathbf{x}_i) \cdot h(p_i; \mu(\mathbf{x}_i)), \quad h(p_i; \mu(\mathbf{x}_i)) = \left( \frac{1}{\mu(\mathbf{x}_i)} p_i^{\frac{1}{\mu(\mathbf{x}_i)} - 1} \right), \quad (6)$$

where  $\mathbf{x}_i \in [0, 1]^{100}$  denotes the side information of the  $i$ th hypothesis,  $\pi(\mathbf{x}_i)$  denotes proportion of the false nulls in the mixture,  $h$  denotes the false null distribution of  $Beta(1/\mu(\mathbf{x}_i), 1)$ . The  $\pi(\mathbf{x}_i)$ ’s and  $\mu(\mathbf{x}_i)$ ’s are determined by the following relationships with the 100-dimensional side information:

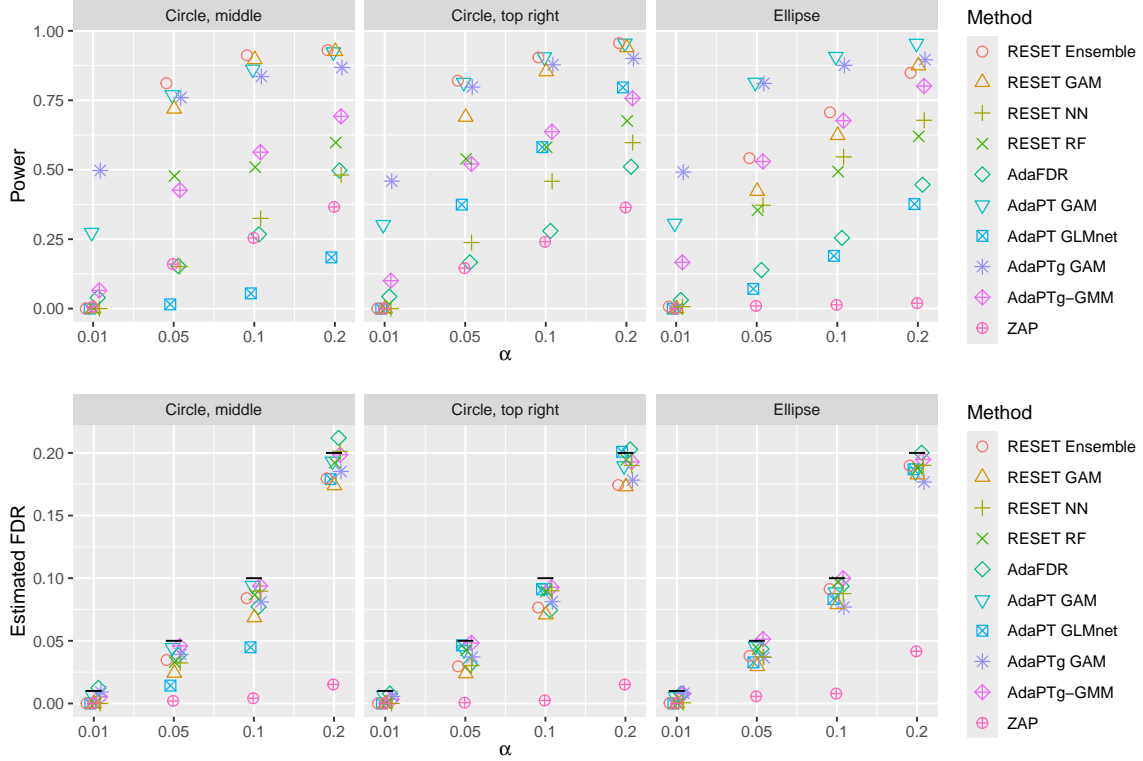


Figure 10: **RESET vs. other methods using two-dimensional side information with p-values.** The first row plots the power and the second row plots the estimated FDR for each FDR threshold ranging from 1% to 20%. Each color and shape combination corresponds to a unique method. The three columns correspond to the hypotheses’ relationship to the side information according to Figure 9. The horizontal segments in the second row of panels mark the corresponding FDR thresholds on the y-axis. For readability, each point is jittered in the horizontal direction.

$$\log\left(\frac{\pi}{1-\pi}\right) = \theta_0 + \mathbf{x}_i^T \theta, \quad \mu_i = \max\{\mathbf{x}_i^T \beta, 1\},$$

where  $\theta = (3, 3, 0, \dots, 0) \in \mathbb{R}^{100}$ ,  $\beta = (2, 2, 0, \dots, 0) \in \mathbb{R}^{100}$  and  $\theta_0$  is chosen to satisfy  $\frac{1}{m} \sum_i \pi(\mathbf{x}_i) = 0.3$ . Clearly, only the first two values in  $\mathbf{x}_i \in [0, 1]^{100}$  contribute to the beta mixture model, as intended. We used 100 independent runs, where in each we drew the 2000 p-values as described.

There were a couple of tools we had to omit from the analysis of this data. Surprisingly, we found that AdaFDR was too slow in this simulation. Similarly, we were not able to apply AdaPT GAM or AdaPT<sub>g</sub> GAM as we did in the previous simulation, since it would have required using a smoothing spline on all 100 side-information variables, which is impractical. Hence, we only applied the GLMnet variants of AdaPT.

Examining Figure 11, which graphically summarizes this analysis, it appears that RESET Ensemble, RESET NN, and AdaPT GLMnet deliver the most discoveries at the 5%, 10%, and 20% FDR levels. At 1% FDR, only AdaPT<sub>g</sub> GLMnet appears to have non-negligible power, albeit a fairly low number of discoveries. Finally, we point out that in this simulation, the model specification of AdaPT/AdaPT<sub>g</sub> perfectly matches the true model. In other words, the fitted mixture model used by AdaPT/AdaPT<sub>g</sub> coincides with Equation (6). Given this, we find it reassuring that RESET Ensemble is still comparable at 5% and higher thresholds.

Notably, the performance of AdaPT in these last two simulation setups is highly dependent on the choice of implementation. In Simulation 5, AdaPT GAM significantly outperforms AdaPT

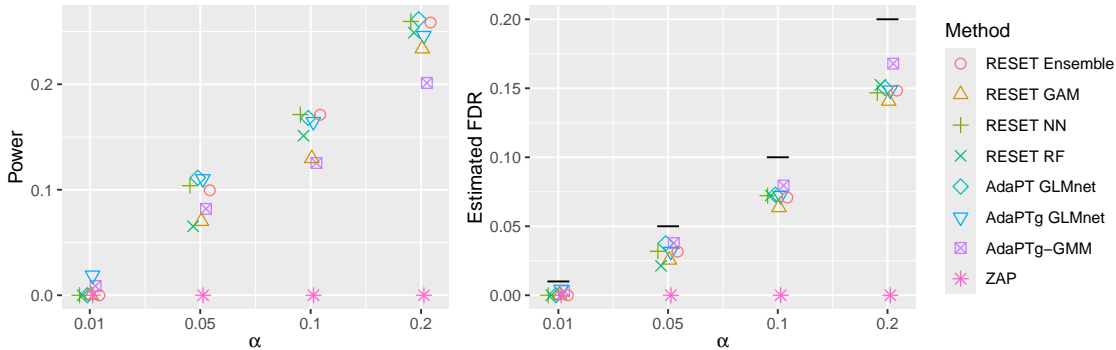


Figure 11: **RESET vs. other methods using 100-dimensional side information with p-values.** The left panel plots the power and the right panel plots the estimated FDR as a function of the FDR thresholds: 1%, 5%, 10% and 20%. Each color and shape combination corresponds to a unique method. The horizontal segments in the right panel mark the corresponding FDR thresholds on the y-axis. For readability, each point is jittered in the horizontal direction.

GLMnet while in Simulation 6, AdaPT GLMnet is superior and AdaPT GAM is not even practical. In contrast, RESET Ensemble selects from a collection of flexible machine learning models to adapt itself to the problem at hand.

## 6.2 Real data experiments with p-values

We next evaluate RESET and related methods on a collection of publicly available datasets with p-values that were investigated by Zhang et al. [51] when introducing AdaFDR and by Lei and Fithian [33] when introducing AdaPT. Since AdaFDR and AdaPT operate under essentially the same assumptions as RESET’s, we expect these datasets to therefore satisfy Assumption 3 with the exception of two datasets, which we discuss at the end of this section. We provide a brief summary of each dataset below.

- Three RNA-seq datasets (Airway [22], Bottomly [4], Pasilla [6]): The goal is to identify genes that are associated with varying gene expression levels in response to a change of conditions. In the Airway data, the differential expression analysis is conducted in response to a drug, dexamethasone; in the Bottomly data, the analysis is conducted between two mouse strains; and in the Pasilla data, the analysis is conducted between normal and so-called ‘Pasilla knockdown’ conditions [23]. In all cases the side information consists of the log-normalized gene counts.
- A proteomics dataset (Proteomics [14]): The goal is to identify proteins that have different protein abundances when treated with rapamycin versus DMSO in yeast cells. Each protein consists of side information equal to the natural log of the number of peptides ‘quantified’ across all samples, i.e., the number of peptides belonging to the protein with their abundances measured.
- Two microbiome datasets (Microbiome Enigma Ph and Microbiome Enigma Al [31, 45]): The goal is to identify microbiome organisms, recorded as OTUs (Operational Taxonomic Units), that are associated with certain conditions (pH and Al). Each hypothesis (OTU) is equipped with a two-dimensional side information — the ubiquity, which is defined as the percentage of samples detected with the OTU, and the mean nonzero abundance, which is defined as the average abundance of each OTU across the samples in which it was detected.

- Two fMRI datasets (Auditory and Imagination) [48]: The goal is to identify voxels that are activated in response to different stimuli. In the first dataset, a single individual received auditory stimulus and in the second dataset, a single individual was instructed to imagine playing tennis. Each hypothesis (voxel) is equipped with four dimensional side information: the spatial position of the voxel (in three dimensions) and a categorical variable with the Brodmann label [5], which is used to delineate different areas of the brain with different functions.
- Two eQTL datasets (Subcutaneous and Omentum [10, 11]): The goal is to identify single nucleotide polymorphisms (SNPs) that are associated with changes in gene expression levels. Such an association is referred to as an expression quantitative trait locus (eQTL). Each hypothesis (SNP) is equipped with the following four side information variables: (1) the distance between the SNP and the gene transcription’s start site (TSS), (2) the log gene expression level, (3) the alternative allele frequency (AAF) of the SNP and (4) the chromatin state of the SNP.
- Gene-drug response data (Estrogen [12, 36]): The goal is to identify genes that are differentially expressed in response to a low-dosage estrogen treatment applied to breast cancer cells. Each hypothesis (gene) is assigned a ‘rank’ that was generated using an analysis of the gene expression levels in response to (1) a high-dosage estrogen treatment and (2) a medium-dosage estrogen treatment. Here, the ranks are in terms of the strength of association between the expression level of each gene and the level of dosage in (1) and (2). Thus, we can analyze the data twice, once for each side information variable based on (1) and (2).

The results of each method applied to the collection of the above datasets is visually summarized in Figure 12. We can clearly see that RESET Ensemble is comparable to the other methods in terms of discoveries. Indeed, to argue this more accurately, we ranked each method across each dataset and at each FDR threshold considered (ties were averaged). Then we calculated the median rank for each method. RESET Ensemble and AdaPT<sub>g</sub>-GMM were tied with the highest median rank. Moreover, for each dataset and each FDR threshold in Figure 12, we computed the maximum number of discoveries across all methods and determined the relative power of each method to this maximum. The boxplots in Figure 13 display the relative powers for each method. Visually, RESET Ensemble and AdaPT<sub>g</sub>-GMM have the highest medians, with RESET Ensemble at 95.9% and AdaPT<sub>g</sub>-GMM at 94.5% with RESET Ensemble’s boxplot edging higher overall.

There are a couple of implementation details we would like to highlight here (for full details, see Supplementary Sections S.6-S.10). First, we used the same default options of RESET Ensemble on all datasets, except for the two fMRI datasets which exhibit a spike of p-values close to 1. In this case, it is sensible to define asymmetric target and decoy regions,  $[0, 0.3)$  and  $(0.3, 0.9]$  respectively as Chao and Fithian [8] did in their application of AdaPT<sub>g</sub>-GMM to this dataset. We also point out that we applied AdaPT<sub>g</sub>-GMM and ZAP using the p-value information rather than the test statistic information (see Section 3.1 for background on these methods). To do so, AdaPT<sub>g</sub>-GMM allows the user to directly input p-values instead of z-statistics. For ZAP, we converted the p-value information into z-values by defining  $z_i = \pm\Phi^{-1}(p_i/2)$  of each p-value,  $p_i$ , where the signs are chosen *i.i.d.* uniformly. In other words, we input plausible z-values that correspond to the same p-value information used by the other tools. As we mentioned in Section 3, our implementation of RESET focuses on the use of p-values, and we leave the extension to test statistic information as part of future work.

To evaluate the computation times for each method, we used the two fMRI datasets, which uses the largest number of side information variables and has a large number of hypotheses. Figure 14(A-



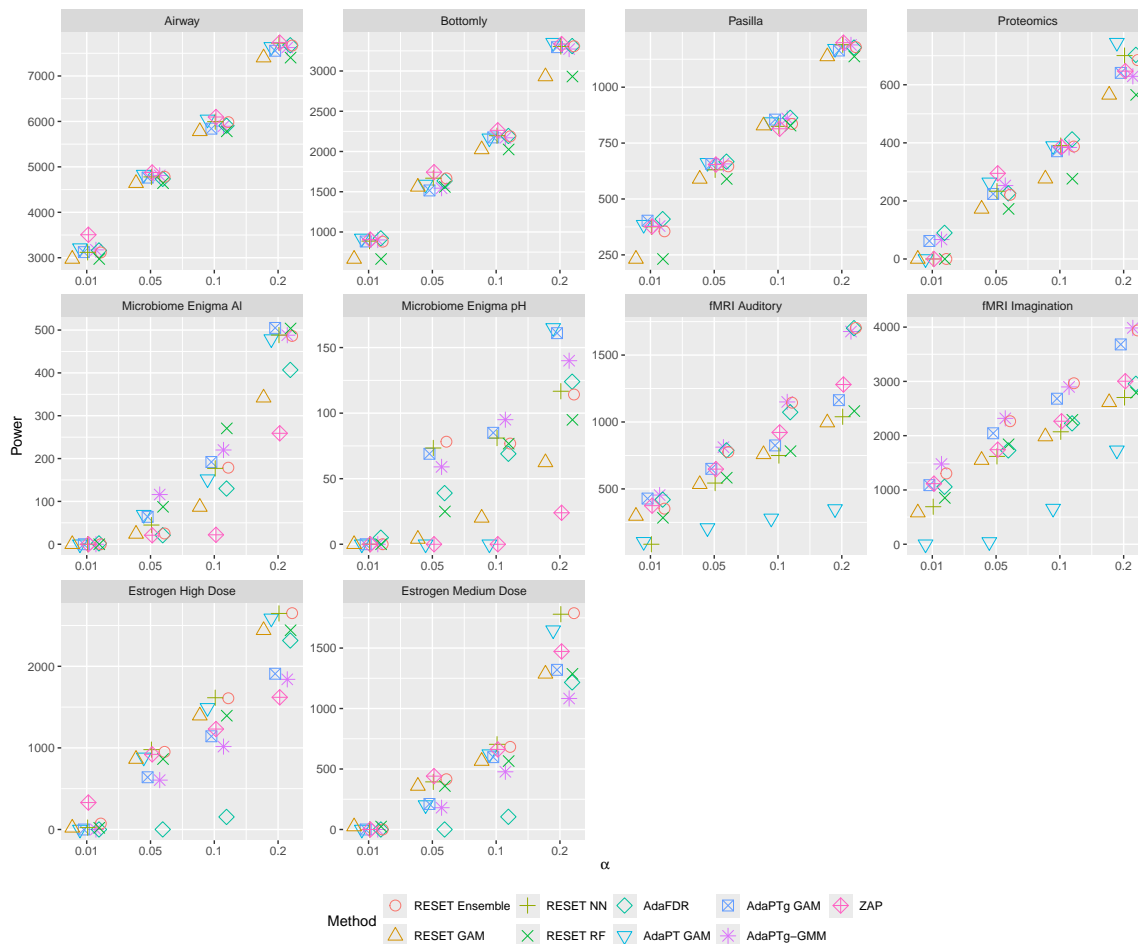


Figure 12: **Comparison of RESET and other methods using a collection of publicly available datasets.** Each method was evaluated at the FDR thresholds of 1%, 5%, 10%, and 20%. The number of discoveries reported by each RESET method is averaged over 10 applications at FDR threshold and dataset. Each color and shape combination corresponds to a unique method. For readability, each point is jittered in the horizontal direction.

B) shows the computation times for each considered method, where the fastest are the collection of RESET methods, ZAP and AdaFDR. RESET NN, RESET GAM and RESET RF are slightly faster than our ensemble approach which considers all of them.

Notably, we have excluded the analysis of the two eQTL studies from Figure 12. This is because this dataset exhibits a high degree of p-value dependency, even among the true null hypotheses and thus violates Assumption 3 which guarantees our type-1 error control. Indeed, this phenomenon is due to *linkage disequilibrium* in which SNPs behave dependently. As a consequence, the dataset exhibits virtually identical copies of the same p-value, with similar side information, even if the p-value is large, suggesting a true null hypothesis. Figure 14(C-D) shows that RESET Ensemble reports substantially more discoveries on these eQTL datasets than all the non-RESET variants. This is because many estimating and training decoys are virtually the same and the random forest is sensitive to this leakage of information. Evidently, RESET NN is more robust to this problem: the number of discoveries is in the same ‘ballpark’ as other methods. Note that RESET GAM shares identical results with RESET RF since it fails to perform a spline basis expansion on one of the side information variables (the chromatin state of the SNP), and so RESET GAM switches to RESET RF in this case.

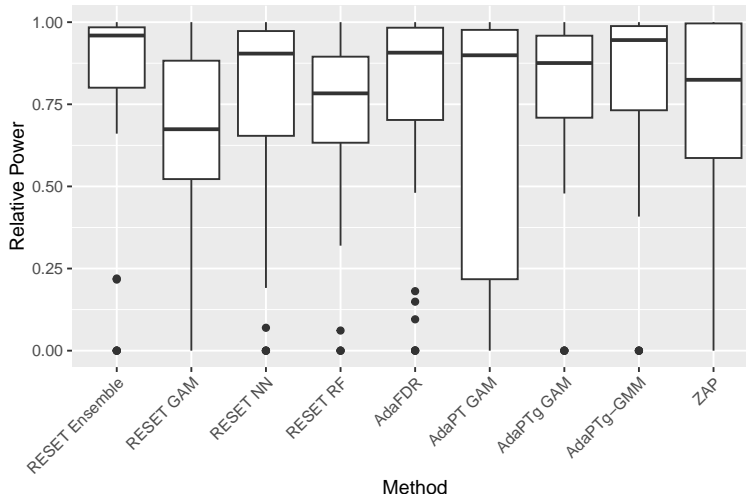


Figure 13: **Relative power of each method.** Each boxplot describes the relative power of each method computed for each dataset and FDR threshold in Figure 12.

### 6.3 FDP control with p-values

In this final section, we demonstrate RESET’s application of FDP control in the p-value setting. Here we define the following asymmetric target and decoy regions,  $[0, 0.3)$  and  $(0.3, 0.9]$  respectively, for *all* datasets. The rationale stems from our later analysis in the Discussion, as well as our comments at the end of Section 5.2.3, which point out that when the ratio of estimating decoys to true null targets is small, the subsequent FDP-SD step in RESET might incur a loss of power. Hence, to rectify this, we essentially double the number of estimating decoys under consideration by defining a decoy region that is twice as large as the corresponding target region.

As far as we can tell, there are no p-value based testing procedures that use side information while controlling the FDP in the sense of Section 2. Hence, we compare RESET to the following generic methods for FDP control. The first of these methods is the previously considered FDP-SD that we analyzed in the competition setting, but adapted for the p-value setup. Each of the labels and scores  $(L, W)$  required for FDP-SD are constructed in the same way as in RESET’s Step 1 (Section 4), where we used the same asymmetric target and decoy regions described above. The second method we compare to is the p-value based analogue called GR-SD [20] (see Section 3).

Figure 15 displays the number of discoveries obtained by each method on the collection of real datasets we considered in the previous section, with varying FDR thresholds (1%, 5%, 10%, 20%) and confidence levels (50%, 80%, 90%). RESET Ensemble is much more powerful than the alternative non-side information approaches with a few exceptions.

## 7 Discussion

We introduced RESET, a flexible wrapper for any semi-supervised learning algorithm. Alongside, we provide an implementation of RESET, called RESET Ensemble, that is power-wise competitive with recently developed methods for competition as well as p-value based multiple testing problems with side information, fast compared to most tools, and flexible as it allows finite-sample of either FDR or FDP control.

In terms of power, we highlight the fact that competing tools, such as the variants of AdaPT or Adaptive Knockoffs, require an initial selection of one of those variants. Making a selection after

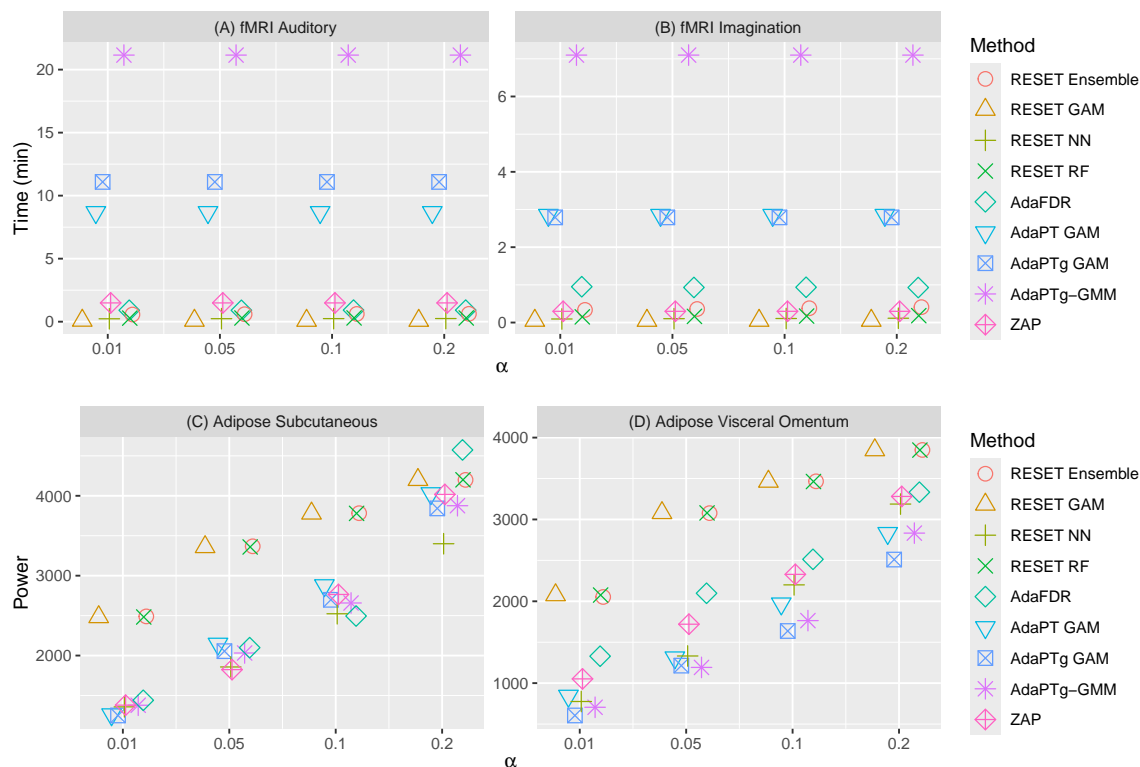


Figure 14: **Comparison of runtime and power.** In (A) and (B), we compare the computation time of each method on the fMRI datasets. We averaged the times of each RESET method over 10 applications. In (C) and (D), we compare the number of discoveries using the two eQTL datasets. The number of discoveries reported by each RESET method is averaged over 10 applications at FDR threshold and dataset. In all panels, we evaluated each method at FDR thresholds of: 1%, 5%, 10%, 20%.

observing the discovery lists of each tool will generally compromise its FDR control. Thus, we compared RESET Ensemble to the default competing method if one was available, which was the case of Adaptive Knockoff’s GAM filter, or *separately* to each variant, which was the case of AdaPT. Based on our comparisons, we conclude that RESET Ensemble is able to achieve comparable or slightly greater power than many of these tools while freeing the user from having to choose the ‘right’ method to begin with.

As far as computational runtime, we found that our collection of RESET methods provide a faster alternative to *all* competing methods with finite FDR control in our considered experiments. The only case in which RESET was surpassed in terms of speed was ZAP-asympt, which demonstrated marginally faster runtimes than RESET Ensemble in one of the fMRI datasets (Figure 14B). However, ZAP-asympt’s fast runtimes come at the cost of asymptotic FDR control. The most striking difference in runtimes was in the peptide detection context using mass spectrometry data, in which all variants of Adaptive Knockoffs were generally too slow to be practical.

Finally, we point out that RESET’s compatibility with FDR or FDP control is unique. In the competition setting, we note that it would be challenging to combine Adaptive Knockoffs with FDP-SD because FDP-SD is a stepdown procedure while Adaptive Knockoffs is essentially a step-up procedure. Katsevich and Ramdas [27] provide a general method for adaptive ordering using their method for simultaneous FDP bounds. However, (a) they do not provide an exact implementation of this, only a theoretical discussion, and (b) their approach is conservative since it controls the FDP at every cutoff (which allows the analyst to explore the nested discovery lists without breaking FDP control). To the best of our knowledge, in the competition framework with side information,

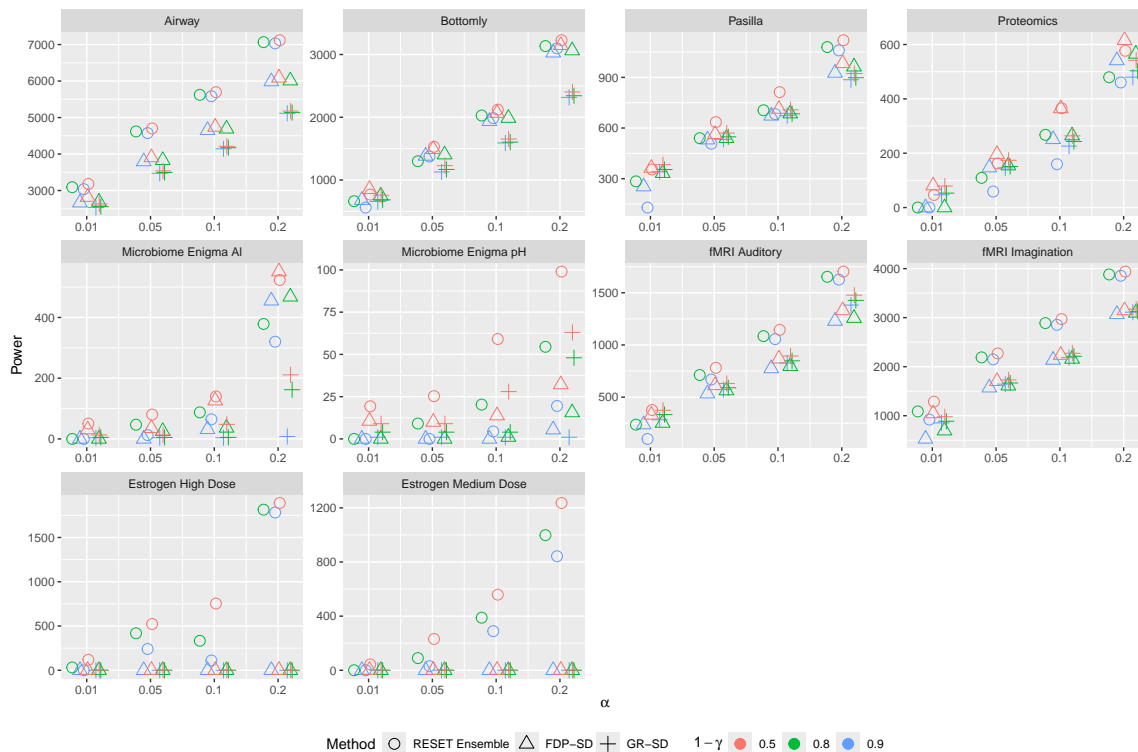


Figure 15: **Comparison of RESET and other methods with FDP control using a collection of publicly available data.** Each panel plots the number of discoveries obtained by RESET Ensemble, FDP-SD and GR-SD at a range of FDR thresholds (1%, 5%, 10%, 20%) with varying confidence  $1 - \gamma$  (0.5, 0.8, 0.9).

RESET is the only method of reordering that may be flexibly used with FDP-SD without the additional cost of (b). Similarly, we know of no method that allows finite sample FDP control in the p-value setting with side information.

On the topic of RESET’s FDP control, we point out the following limitation. When the number of discoveries is small, e.g., when the confidence is too high, RESET may yield less power, even if the side information is reasonably informative. To illustrate this phenomenon, we computed the bounds,  $\delta_i$  on the number of decoy wins in the top  $i$  scores from Algorithm S2, which are used to determine the reported list of discoveries in FDP-SD (with  $c = 1/2$ ) and RESET (using the default  $c = 2/3$ ). We considered a confidence level of  $1 - \gamma = 90\%$  and an FDP threshold of  $\alpha = 1\%$ . Since we removed approximately half the decoys for training purposes in RESET, the bounds need to be doubled to fairly compare between the two approaches.

Figure 16 shows the bounds for FDP-SD, and double the bounds for RESET, along with the ratio of the two at a range of different indices. We can see that for smaller indices, this ratio is much smaller, initially at 0% at an index of 501 and 50% at an index of 1K, while at 10K this ratio is much higher at 94%. If the order of the hypotheses is the same, then RESET’s smaller bounds imply it will report fewer discoveries because RESET employs FDP-SD to control the FDP by searching for the largest index  $i$  s.t.  $D_{i_0} \leq \delta_i, \dots, D_i \leq \delta_i$ , and reports the top  $i$  scoring positively labeled hypotheses. In other words, if RESET is to report roughly the same number of discoveries as FDP-SD, then RESET needs to rearrange the targets and estimating decoys successfully enough so as to make up for a 50% difference in the bounds when considering the top 1K scores, while only 6% when considering the top 10K. If the side information is not rich enough, then it is possible RESET will report few discoveries than FDP-SD in these cases. We intend to investigate this as

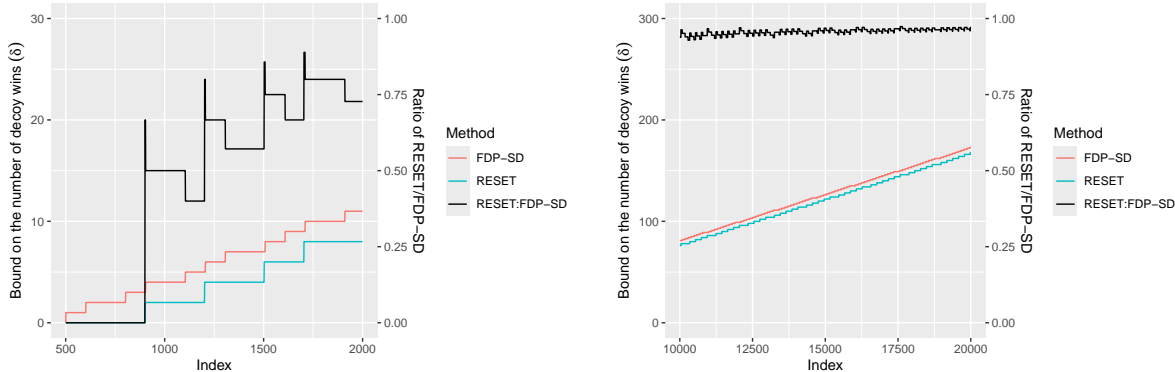


Figure 16: **RESET’s and FDP-SD’s bounds on the number of decoy wins.** We recorded, on the left y-axis, the bounds used to determine the list of FDP-SD discoveries and twice the bounds used to determine RESET’s discoveries at a range of indices at  $\alpha = 1\%$  and  $1 - \gamma = 90\%$ . On the right y-axis, we plot the ratio of these bounds (in black). The left panel looks at indices between 501 to 2K, while the right panel looks at indices from 10K to 20K. An index corresponds to the number of top scoring hypotheses (regardless of their labels).

part of future work.

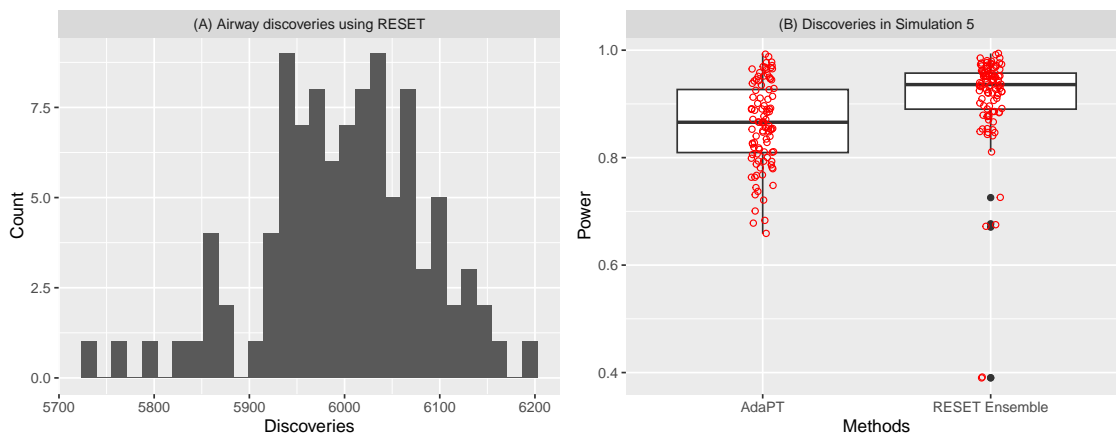


Figure 17: **Variability in the number of discoveries.** in the Airway data and in Simulation 5 (A) Histogram of the number of RESET Ensemble discoveries applied 100 times to the Airway data with a 10% FDR threshold and varying its internal seed. (B) Boxplots of RESET’s and AdaPT’s power in 100 applications of the ‘circle in the middle’ setup of Simulation 5 using a 10% FDR threshold. There are two outliers in RESET’s case (which occurred when the signal was considerably low).

Notably, RESET’s discovery list is variable since it randomly splits the decoys into two sets: one set for training and the other for estimating the false discoveries. This variability is demonstrated in the histogram of the number of discoveries in Figure 17A using 100 applications of RESET Ensemble to the Airway dataset at an FDR threshold of 10%. The resulting number of discoveries has a mean of 5998 with a standard deviation of about 85. While this is problematic to an extent, keep in mind that the data distribution is random, and the added variance from RESET may be marginal at times. Indeed, in Figure 17(B), we find that in the case of Simulation 5 from Section 6.1.1, RESET is overall arguably less variable than AdaPT, even though AdaPT does not employ any internal randomization. In practice, users may get around RESET’s randomization by setting the random number generator to be a function of the input data and parameters. We plan on adding this feature to a future update.

Lastly, while RESET is a flexible method for the competition and p-value based testing, we wish

to further extend it to the test-statistic setting. There is more than one way of generalizing RESET to accommodate a test statistic  $z_i$  for each hypothesis  $H_i$ . Moreover, there are several ‘types’ of interactions between the side information  $\mathbf{x}_i$  and the test statistic  $z_i$  which are not preserved when switching to p-values, as outlined by Leung and Sun [35]. Thus it is not clear that RESET Ensemble will be equally applicable in this setting without substantial modifications.

## References

- [1] R. F. Barber and Emmanuel J. Candès. Controlling the false discovery rate via knockoffs. *The Annals of Statistics*, 43(5):2055–2085, 2015.
- [2] Y. Benjamini and Y. Hochberg. Controlling the false discovery rate: a practical and powerful approach to multiple testing. *Journal of the Royal Statistical Society Series B*, 57:289–300, 1995.
- [3] Y. Benjamini, A. M. Krieger, and D. Yekutieli. Adaptive linear step-up procedures that control the false discovery rate. *Biometrika*, 93(3):491–507, 2006.
- [4] Daniel Bottomly, Nicole AR Walter, Jessica Ezzell Hunter, Priscila Darakjian, Sunita Kawane, Kari J Buck, Robert P Searles, Michael Mooney, Shannon K McWeeney, and Robert Hitzemann. Evaluating gene expression in c57bl/6j and dba/2j mouse striatum using rna-seq and microarrays. *PLoS one*, 6(3):e17820, 2011.
- [5] Korbinian Brodmann. *Vergleichende Lokalisationslehre der Grosshirnrinde in ihren Prinzipien dargestellt auf Grund des Zellenbaues*. Barth, 1909.
- [6] Angela N Brooks, Li Yang, Michael O Duff, Kasper D Hansen, Jung W Park, Sandrine Dudoit, Steven E Brenner, and Brenton R Graveley. Conservation of an rna regulatory map between drosophila and mammals. *Genome research*, 21(2):193–202, 2011.
- [7] E. J. Candès, Y. Fan, L. Janson, and J. Lv. Panning for gold: Model-X knockoffs for high-dimensional controlled variable selection. *Journal of the Royal Statistical Society: Series B (Statistical Methodology)*, 80(3):551–577, 2018.
- [8] Patrick Chao and William Fithian. Adapt-gmm: Powerful and robust covariate-assisted multiple testing. *arXiv preprint arXiv:2106.15812*, 2021.
- [9] J. M. Chick, D. Kolippakkam, D. P. Nusinow, B. Zhai, R. Rad, E. L. Huttlin, and S. P. Gygi. A mass-tolerant database search identifies a large proportion of unassigned spectra in shotgun proteomics as modified peptides. *Nature Biotechnology*, 33(7):743–749, 2015.
- [10] GTEx Consortium. The gtex consortium atlas of genetic regulatory effects across human tissues. *Science*, 369(6509):1318–1330, 2020.
- [11] GTEx Consortium, Kristin G Ardlie, David S Deluca, Ayellet V Segrè, Timothy J Sullivan, Taylor R Young, Ellen T Gelfand, Casandra A Trowbridge, Julian B Maller, Taru Tukiainen, et al. The genotype-tissue expression (gtex) pilot analysis: multitissue gene regulation in humans. *Science*, 348(6235):648–660, 2015.
- [12] Sean Davis and Paul S Meltzer. Geoquery: a bridge between the gene expression omnibus (geo) and bioconductor. *Bioinformatics*, 23(14):1846–1847, 2007.
- [13] A. P. Dempster, N. M. Laird, and D. B. Rubin. Maximum likelihood from incomplete data via the EM algorithm. *Journal of the Royal Statistical Society. Series B (Methodological)*, 39:1–22, 1977.
- [14] Noah Dephoure and Steven P Gygi. Hyperplexing: a method for higher-order multiplexed quantitative proteomics provides a map of the dynamic response to rapamycin in yeast. *Science signaling*, 5(217):rs2–rs2, 2012.

- [15] B. Diament and W. S. Noble. Faster SEQUEST searching for peptide identification from tandem mass spectra. *Journal of Proteome Research*, 10(9):3871–3879, 2011.
- [16] A. Ebadi, D. Luo, J. Freestone, W. S. Noble, and Uri Keich. Bounding the FDP in competition-based control of the FDR. *arXiv preprint arXiv:2302.11837*, 2023.
- [17] J. E. Elias and S. P. Gygi. Target-decoy search strategy for increased confidence in large-scale protein identifications by mass spectrometry. *Nature Methods*, 4(3):207–214, 2007.
- [18] Jack Freestone, William S Noble, and Uri Keich. Analysis of tandem mass spectrometry data with conga: Combining open and narrow searches with group-wise analysis. *Journal of Proteome Research*, 23(6):1894–1906, 2024.
- [19] Jelle J. Goeman, Jesse Hemerik, and Aldo Solari. Only closed testing procedures are admissible for controlling false discovery proportions. *The Annals of Statistics*, 49(2):1218 – 1238, 2021.
- [20] Wenge Guo and Joseph Romano. A generalized sidak-holm procedure and control of generalized error rates under independence. *Statistical applications in genetics and molecular biology*, 6(1), 2007.
- [21] K. He, Y. Fu, W.-F. Zeng, L. Luo, H. Chi, C. Liu, L.-Y. Qing, R.-X. Sun, and S.-M. He. A theoretical foundation of the target-decoy search strategy for false discovery rate control in proteomics. *arXiv*, 2015. <https://arxiv.org/abs/1501.00537>.
- [22] Blanca E Himes, Xiaofeng Jiang, Peter Wagner, Ruoxi Hu, Qiyu Wang, Barbara Klanderma, Reid M Whitaker, Qingling Duan, Jessica Lasky-Su, Christina Nikolos, et al. Rna-seq transcriptome profiling identifies crispld2 as a glucocorticoid responsive gene that modulates cytokine function in airway smooth muscle cells. *PloS one*, 9(6):e99625, 2014.
- [23] W. Huber and A. Reyes. pasilla: Data package with per-exon and per-gene read counts of rna-seq samples of pasilla knock-down by brooks et al., genome research 2011, r package 1.34.0.
- [24] Nikolaos Ignatiadis and Wolfgang Huber. Covariate powered cross-weighted multiple testing. *Journal of the Royal Statistical Society Series B: Statistical Methodology*, 83(4):720–751, 2021.
- [25] Nikolaos Ignatiadis, Bernd Klaus, Judith B Zaugg, and Wolfgang Huber. Data-driven hypothesis weighting increases detection power in genome-scale multiple testing. *Nature methods*, 13(7):577–580, 2016.
- [26] L. Käll, J. D. Canterbury, J. Weston, W. S. Noble, and Michael J MacCoss. Semi-supervised learning for peptide identification from shotgun proteomics datasets. *Nature Methods*, 4(11):923–925, 2007.
- [27] E. Katsevich and A. Ramdas. Simultaneous high-probability bounds on the false discovery proportion in structured, regression and online settings. *The Annals of Statistics*, 48(6):3465 – 3487, 2020.
- [28] A. Keller, A. I. Nesvizhskii, E. Kolker, and R. Aebersold. Empirical statistical model to estimate the accuracy of peptide identification made by MS/MS and database search. *Analytical Chemistry*, 74:5383–5392, 2002.



- [29] A. Kertesz-Farkas, F. L. Nii Adoquaye Acquaye, K. Bhimani, J. K. Eng, W. E. Fondrie, C. Grant, M. R. Hoopmann, A. Lin, Y. Y. Lu, R. L. Moritz, M. J. MacCoss, and W. S. Noble. The Crux Toolkit for Analysis of Bottom-Up Tandem Mass Spectrometry Proteomics Data. *Journal of Proteome Research*, 22(2):561–569, Feb 2023.
- [30] A. T. Kong, F. V. Leprevost, D. M. Avtonomov, D. Mellacheruvu, and A. I. Nesvizhskii. MSFragger: ultrafast and comprehensive peptide identification in mass spectrometry-based proteomics. *Nature Methods*, 14(5):513–520, 2017.
- [31] Keegan Korthauer, Patrick K Kimes, Claire Duvallet, Alejandro Reyes, Ayshwarya Subramanian, Mingxiang Teng, Chinmay Shukla, Eric J Alm, and Stephanie C Hicks. A practical guide to methods controlling false discoveries in computational biology. *Genome biology*, 20:1–21, 2019.
- [32] M. R. Lazear. Sage: An open-source tool for fast proteomics searching and quantification at scale. *Journal of Proteome Research*, 22(11):3652–3659, 2023.
- [33] L. Lei and W. Fithian. Adapt: an interactive procedure for multiple testing with side information. *Journal of the Royal Statistical Society: Series B (Statistical Methodology)*, 80(4):649–679, 2018.
- [34] Lihua Lei, Aaditya Ramdas, and William Fithian. Star: A general interactive framework for fdr control under structural constraints. *arXiv preprint arXiv:1710.02776*, 2017.
- [35] D. Leung and W. Sun. Zap: z-value adaptive procedures for false discovery rate control with side information. *Journal of the Royal Statistical Society Series B: Statistical Methodology*, 84(5):1886–1946, 2022.
- [36] Ang Li and Rina Foygel Barber. Accumulation tests for fdr control in ordered hypothesis testing. *Journal of the American Statistical Association*, 112(518):837–849, 2017.
- [37] Ang Li and Rina Foygel Barber. Multiple testing with the structure-adaptive benjamini–hochberg algorithm. *Journal of the Royal Statistical Society Series B: Statistical Methodology*, 81(1):45–74, 2019.
- [38] Jinzhou Li, Marloes H Maathuis, and Jelle J Goeman. Simultaneous false discovery proportion bounds via knockoffs and closed testing. *arXiv preprint arXiv:2212.12822*, 2022.
- [39] A. Lin, T. Short, W. S. Noble, and U. Keich. Improving peptide-level mass spectrometry analysis via double competition. *Journal of Proteome Research*, 21(10):2412–2420, 2022.
- [40] Dong Luo, Arya Ebadi, Kristen Emery, Yilun He, William Stafford Noble, and Uri Keich. Competition-based control of the false discovery proportion. *Biometrics*, 2023. In press.
- [41] L. Martens, H. Hermjakob, P. Jones, M. Adamsk, C. Taylor, D. States, K. Gevaert, J. Vandekerckhove, and R. Apweiler. PRIDE: The proteomics identifications database. *Proteomics*, 5(13):3537–3545, 2005.
- [42] A. I. Nesvizhskii. A survey of computational methods and error rate estimation procedures for peptide and protein identification in shotgun proteomics. *Journal of Proteomics*, 73(11):2092–2123, 2010.

- [43] C. Y. Park, A. A. Klammer, L. Käll, M. P. MacCoss, and W. S. Noble. Rapid and accurate peptide identification from tandem mass spectra. *Journal of Proteome Research*, 7(7):3022–3027, 2008.
- [44] Z. Ren and E. Candès. Knockoffs with side information. *The Annals of Applied Statistics*, 17(2):1152–1174, 2023.
- [45] Mark B Smith, Andrea M Rocha, Chris S Smillie, Scott W Olesen, Charles Paradis, Liyou Wu, James H Campbell, Julian L Fortney, Tonia L Mehlhorn, Kenneth A Lowe, et al. Natural bacterial communities serve as quantitative geochemical biosensors. *MBio*, 6(3):10–1128, 2015.
- [46] J. D. Storey, J. E. Taylor, and D. Siegmund. Strong control, conservative point estimation, and simultaneous conservative consistency of false discovery rates: A unified approach. *Journal of the Royal Statistical Society, Series B*, 66:187–205, 2004.
- [47] P. Sulimov and A. Kertész-Farkas. Tailor: A nonparametric and rapid score calibration method for database search-based peptide identification in shotgun proteomics. *Journal of Proteome Research*, 19(4):1481–1490, 2020.
- [48] Karsten Tabelow and Jörg Polzehl. Statistical parametric maps for functional mri experiments in r: The package fmri. *Journal of Statistical Software*, 44:1–21, 2011.
- [49] R. J. Tibshirani. Regression shrinkage and selection via the lasso. *Journal of the Royal Statistical Society B*, 58(1):267–288, 1996.
- [50] F. Yu, G. C. Teo, A. T. Kong, S. E. Haynes, D. M. Avtonomov, D. J. Geiszler, and A. I. Nesvizhskii. Identification of modified peptides using localization-aware open search. *Nature Communications*, 11(1):4065, August 2020.
- [51] Martin J Zhang, Fei Xia, and James Zou. Fast and covariate-adaptive method amplifies detection power in large-scale multiple hypothesis testing. *Nature communications*, 10(1):3433, 2019.

# Supplement

## S.1 Algorithms

---

**Algorithm S1 Selective SeqStep / SeqStep+** (adopted from Selective Sequential Step+ of [1])

---

**Input:**

- $(L_i, W_i)_{i=1}^m$  the list of paired winning labels and scores;
- $c \in (0, 1)$  - the probability of a null target/feature win;
- $\alpha \in (0, 1)$  - the FDR threshold;

**Output:** A discovery list  $R_\alpha$

- 1: sort the paired  $(L_i, W_i)$  in decreasing order of  $W_i$  ▷ ties are randomly broken
  - 2:  $D_k \leftarrow \#\{i \leq k : L_i = -1\}$  ▷ number of decoy/knockoffs wins in top  $k$  scores
  - 3:  $T_k \leftarrow \#\{i \leq k : L_i = 1\}$  ▷ number of target/original feature wins in top  $k$  scores
  - 4: **if** SeqStep **then**
  - 5:      $k_0 \leftarrow \max\{k : \frac{D_k}{T_k \vee 1} \cdot \frac{c}{1-c} \leq \alpha\}$
  - 6: **else if** SeqStep+ **then**
  - 7:      $k_0 \leftarrow \max\{k : \frac{D_k+1}{T_k \vee 1} \cdot \frac{c}{1-c} \leq \alpha\}$
  - 8: **end if**
  - 9: **return**  $R_\alpha \leftarrow \{i : \text{the (pre-sorted) } W_i \text{ is in the top } k_0 \text{ ranks and } L_i = 1\}$
-

---

**Algorithm S2 FDP-SD** (adopted from [40])

---

**Input:** •  $(L_i, W_i)_{i=1}^m$  the list of paired winning labels and scores;  
•  $c \in (0, 1)$  - the probability of a null target/feature win;  
•  $\alpha \in (0, 1)$  - the FDP threshold;  
•  $\gamma \in (0, 1)$  - for a  $1 - \gamma$  confidence level;

**Output:** A discovery list  $R_{\alpha, \gamma}$

```
1: sort the paired  $(L_i, W_i)$  in decreasing order of  $W_i$  ▷ ties are randomly broken
2:  $\lambda \leftarrow 1 - c$  ▷ the probability of a null decoy win
3:  $R \leftarrow (1 - \lambda)/(c + 1 - \lambda)$ 
4:  $i_0 \leftarrow \max\{1, \lceil (\lceil \log_{1-R}(\gamma) \rceil) / \alpha \rceil\}$ 
5: for  $i = i_0, \dots, m$  do
6:    $D_i \leftarrow \#\{j \leq i : L_j = -1\}$  ▷ number of decoy wins in top  $i$  scores
7:    $\delta_i \leftarrow \max\{d \in \{0, 1, \dots, i\} : F_{B(\lfloor (i-d)\alpha + 1 + d, R \rfloor)}(d) \leq \gamma\}$  ▷  $F_{B(n,p)}$  denotes the CDF of a Binomial( $n, p$ ) RV
8: end for
9:  $i \leftarrow i_0$  and  $\delta_{i_0-1} \leftarrow -1$  and  $\bar{\delta}_{i_0-1} \leftarrow 0$ 
10: while  $i \leq m$  do
11:    $k_0 \leftarrow \lfloor (i - \delta_i) \cdot \alpha \rfloor + 1$ 
12:    $k_1 \leftarrow \lfloor (i - \delta_i + 1) \cdot \alpha \rfloor + 1$ 
13:    $p_0 \leftarrow F_{B(k_0 + \delta_i, R)}(\delta_i)$ 
14:    $p_1 \leftarrow F_{B(k_1 + \delta_i + 1, R)}(\delta_i + 1)$ 
15:    $w_i \leftarrow (p_1 - \gamma)/(p_1 - p_0)$ 
16:   if  $\bar{\delta}_{i-1} = \delta_i + 1$  then
17:      $\bar{\delta}_i \leftarrow \bar{\delta}_{i-1}$ 
18:   else
19:     if  $\delta_i > \delta_{i-1}$  then
20:        $w' \leftarrow w_i$ 
21:     else
22:        $w' \leftarrow w_i / w_{i-1}$ 
23:     end if
24:   end if
25:   Randomly set  $\bar{\delta}_i \leftarrow \delta_i$  or  $\bar{\delta}_i \leftarrow \delta_i + 1$  with probabilities  $w'$  and  $1 - w'$  respectively
26:   if  $D_i \leq \bar{\delta}_i$  then
27:      $i \leftarrow i + 1$ 
28:   else
29:     break
30:   end if
31: end while
32: if  $D_{i_0} \leq \bar{\delta}_{i_0}$  then
33:    $k_{FDP} \leftarrow i - 1$ 
34: else
35:    $k_{FDP} \leftarrow 0$ 
36: end if
37:  $R_{\alpha, \gamma} \leftarrow \{i : \text{the (pre-sorted) } W_i \text{ is in the top } k_{FDP} \text{ ranks and } L_i = 1\}$ 
```

---

---

**Algorithm S3 GR-SD** (adopted from [20])

---

- Input:**
- $(p_i)_{i=1}^m$  the list of p-values;
  - $\alpha \in (0, 1)$  - the FDP threshold;
  - $\gamma \in (0, 1)$  - for a  $1 - \gamma$  confidence level;

**Output:** A discovery list  $R_{\alpha, \gamma}$

- 1: sort the p-values  $(p_i)$  in ascending order ▷ ties are randomly broken
  - 2: **for**  $i = 1, \dots, m$  **do**
  - 3:      $k_i \leftarrow \lfloor \alpha i \rfloor + 1$
  - 4:      $\delta_i \leftarrow F^{-1}[k_i, m - i + 1](\gamma)$  ▷  $F^{-1}[\alpha, \beta](\cdot)$  denotes the CDF of a Beta( $\alpha, \beta$ ) RV
  - 5: **end for**
  - 6:  $k_{GR} \leftarrow \max\{i : \prod_{j=1}^i 1_{p_j \leq \delta_j} = 1 \text{ or } i = 0\}$
  - 7:  $R_{\alpha, \gamma} \leftarrow \{i \in [m] : i \leq k_{GR}\}$
- 

---

**Algorithm S4 RESET**

---

- Input:**
- $\{(L_i, W_i, \mathbf{x}_i) : i = 1, \dots, m\}$  - each hypothesis' (label, winning score, side information);
  - $\alpha$  - FDR threshold for the discovery list;
  - $s$  - the probability of assigning a decoy to the training set (default:  $s = 1/2$ );
  - $f$  - a semi-supervised machine learning model;
  - $c_0$  - an upper bound probability for a true null label  $\mathbb{P}(L_i = 1) \leq c_0$  ( $i$  is a true null);
  - **isFDR** - a boolean which determines whether FDR or FDP control is desired;
  - $\gamma$  - a confidence parameter if FDP control is desired;

**Output:** A discovery list  $R$

- 1:  $I \leftarrow$  a subset of the decoy win indices,  $\{i : L_i = -1\}$ , determined by randomly including each one with probability  $s$
  - 2:  $\tilde{L}_i \leftarrow -1$  for  $i \in I$  ▷ training decoys
  - 3:  $\tilde{L}_i \leftarrow 1$  for  $i \in J := I^c$  ▷ pseudo-targets
  - 4:  $(\tilde{W}_i)_{i=1}^m \leftarrow f\left((W_i, U_i, \tilde{L}_i)_{i=1}^m\right)$  ▷ where  $f$  is any machine learning model
  - 5: **if** **isFDR** **then**
  - 6:      $R \leftarrow \text{SSS}+((\tilde{W}_i, L_i)_{i \in J}, c = \frac{c_0}{1-s \cdot (1-c_0)}, \alpha)$  ▷ Selective SeqStep+
  - 7: **else**
  - 8:      $R \leftarrow \text{FDP-SD}((\tilde{W}_i, L_i)_{i \in J}, c = \frac{c_0}{1-s \cdot (1-c_0)}, \alpha, \gamma)$  ▷ FDP-stepdown
  - 9: **end if**
  - 10: **return**  $R$
-

## S.2 Proof of Lemma 1 in the main text

We first remind the reader of the Lemma's statement.

**Assumption 3.** *Let  $N$  be the indices of the true null hypotheses. The labels  $\{L_i : i \in N\}$  are i.i.d.  $\pm 1$  random variables with  $\mathbb{P}(L_i = 1) \leq c_0$  and are independent of all the scores  $W$ , the side information  $\mathbf{x}$ , and the labels of the false null hypotheses.*

**Lemma 1** (Chao and Fithian). *Assume that the true null p-values have a non-decreasing density and that they are mutually independent and that they are independent of the false null p-values as well as of all the side information. Then Assumption 3 is satisfied with  $c_0 = \frac{a}{a+b_2-b_1}$ .*

*Proof of Lemma 4.1.* Let  $W$  be all the scores,  $\mathbf{x}$  be all the side information, and  $L_{-i}$  be all the other labels that are not  $L_i$ . Then for a true null p-value,  $p_i$ :

$$\begin{aligned} \mathbb{P}(L_i = 1 \mid W, \mathbf{x}, L_{-i}) &= \frac{\mathbb{P}(p_i \in [0, a] \mid W, \mathbf{x}, L_{-i})}{\mathbb{P}(p_i \in [0, a] \mid W, \mathbf{x}, L_{-i}) + \mathbb{P}(p_i \in (b_1, b_2] \mid W, \mathbf{x}, L_{-i})} \\ &\leq \frac{\mathbb{P}(p_i \in [0, a] \mid W, \mathbf{x}, L_{-i})}{\mathbb{P}(p_i \in [0, a] \mid W, \mathbf{x}, L_{-i}) + \mathbb{P}(p_i \in [0, a] \mid W, \mathbf{x}, L_{-i}) \cdot \frac{b_2-b_1}{a}} \\ &= \frac{a}{a + b_2 - b_1}, \end{aligned}$$

where the first line follows since the denominator sums to 1, and the second line clearly follows from the non-decreasing property as explained next.

First, note that the non-decreasing density property implies that:

$$\mathbb{P}(p_i \in B) \leq \frac{a}{b_2 - b_1} \cdot \mathbb{P}(p_i \in q(B)),$$

where  $B \subseteq [0, a]$  is measurable,  $p_i$  is a true null p-value and  $q$  denotes the inverse transformation of the mirrored p-values that map p-values in  $(b_1, b_2]$  onto  $[0, a)$ , that is  $q(p) := b_2 - \frac{b_2-b_1}{a} \cdot p$ .

Let  $A \subseteq \mathbb{R}$  be measurable and let  $B \subseteq [0, a)$  be such that  $\{W_i \in A\} = \{p_i \in B\} \cup \{p_i \in q(B)\}$ . Then,

$$\begin{aligned} \int_{W_i \in A} 1_{p_i \in [0, a]} dP &= \int 1_{\{p_i \in [0, a] \cap B\}} dP = \mathbb{P}(p_i \in B) \\ &\leq \frac{a}{b_2 - b_1} \mathbb{P}(p_i \in q(B)) \\ &= \frac{a}{b_2 - b_1} \int 1_{\{p_i \in (b_1, b_2] \cap q(B)\}} dP \\ &= \frac{a}{b_2 - b_1} \int_{W_i \in A} 1_{p_i \in (b_1, b_2]} dP, \end{aligned}$$

It follows that:

$$\begin{aligned} \mathbb{P}(p_i \in [0, a] \mid W, \mathbf{x}, L_{-i}) &= \mathbb{P}(p_i \in [0, a] \mid W_i) \\ &\leq \frac{a}{b_2 - b_1} \mathbb{P}(p_i \in (b_1, b_2] \mid W_i) = \frac{a}{b_2 - b_1} \mathbb{P}(p_i \in (b_1, b_2] \mid W, \mathbf{x}, L_{-i}). \end{aligned}$$

□

### S.3 RESET controls the FDR or FDP

In this section we prove that given Assumption 3 RESET controls the FDR or the FDP. We use the target-decoy terminology to refer to a positive label  $L_i = 1$  as a target win or simply a target, and a negative label  $L_i = -1$  as a decoy win or decoy.

**Lemma S1.** *Let  $\tilde{L}_i$  for  $i \in [p]$  denote the pseudo labels, where  $\tilde{L}_i = -1$  for a training decoy and  $\tilde{L}_i = 1$  for a pseudo-target. Let  $\mathcal{F}$  be the sigma-algebra generated by the winning scores  $W$ , the side information  $\mathbf{x}$ , and the labels of the false nulls. Let  $N$  be the indices of the true nulls, and  $L_{-i}, \tilde{L}_{-i}$  be the corresponding labels without the  $i$ th one. Then under Assumption 3, we have for  $i \in N$ ,  $L_i = \pm 1$  with*

$$\mathbb{P}(L_i = +1 \mid \tilde{L}_i = 1) \leq \frac{c_0}{1 - s \cdot (1 - c_0)}, \quad \mathbb{P}(L_i = -1 \mid \tilde{L}_i = 1) \geq \frac{(1 - c_0) \cdot (1 - s)}{1 - s \cdot (1 - c_0)},$$

independently of  $\mathcal{F}, \tilde{L}_{-i}, L_{-i}$ .

*Proof.* By Assumption 3, we know  $\{L_i : i \in N\}$  are i.i.d with  $P(L_i = 1) \leq c_0$ , independently of  $\mathcal{G} := \sigma(\mathcal{F}, \tilde{L}_{-i}, L_{-i})$ . Hence, the following probability statements are independent of  $\mathcal{G}$ . In addition, since each decoy is randomly assigned to the training decoy set independently of anything else with probability  $s$ , for each  $i \in N$  we have:

$$\begin{aligned} \mathbb{P}(L_i = -1, \tilde{L}_i = 1) &= \mathbb{P}(L_i = -1) \cdot \mathbb{P}(\tilde{L}_i = 1 \mid L_i = -1) \\ &\geq (1 - c_0) \cdot (1 - s), \end{aligned}$$

Hence,

$$\begin{aligned} \mathbb{P}(L_i = -1 \mid \tilde{L}_i = 1) &= \frac{\mathbb{P}(L_i = -1, \tilde{L}_i = 1)}{P(\tilde{L}_i = 1)} \\ &\geq \frac{(1 - c_0) \cdot (1 - s)}{(1 - s) \cdot \mathbb{P}(L_i = -1) + 1 \cdot \mathbb{P}(L_i = 1)} \\ &= \frac{(1 - c_0) \cdot (1 - s)}{1 - s \cdot \mathbb{P}(L_i = -1)} \\ &\geq \frac{(1 - c_0) \cdot (1 - s)}{1 - s \cdot (1 - c_0)}. \end{aligned}$$

The proof is complete noting that  $\frac{c_0}{1 - s \cdot (1 - c_0)} + \frac{(1 - c_0) \cdot (1 - s)}{1 - s \cdot (1 - c_0)} = 1$  and  $L_i \in \{\pm 1\}$  a.s.  $\square$

*Remark 1.* Lemma S1 essentially states that the labels  $L_i$  for  $i \in N$  with  $\tilde{L}_i = 1$  are *i.i.d.* random variables with  $\mathbb{P}(L_i = +1) \leq \frac{c_0}{1 - s \cdot (1 - c_0)}$  independently of all other information: the scores  $W$ , the side information  $\mathbf{x}$ , the labels of the false null discoveries, and all the labels  $\tilde{L}$ .

**Theorem 1.** *Under Assumption 3 RESET controls the FDR at the user-specified threshold  $\alpha$ .*

*Proof.* We rely on Theorem 3 of Barber and Candès [1] applied to the set of pseudo-targets ( $\tilde{L}_i = 1$ ) ordered in decreasing order of the learned scores  $\tilde{W}_i$ . Specifically, we assign to each pseudo-target a one-bit p-value:

$$\tilde{p}_i = \begin{cases} \frac{c_0}{1 - s \cdot (1 - c_0)} & L_i = +1 \\ 1 & L_i = -1 \end{cases}.$$

Recall that the scores  $\tilde{W}$  are themselves a function of the values  $(\tilde{L}, W, x)$  and clearly the one bit p-values are a function of the labels  $L_i$ . Then it follows from the last Lemma that given the scores  $\tilde{W}$  and the one-bit p-values of the false nulls, the one-bit p-values of the true nulls hypotheses ( $i \in N$  with  $\tilde{L}_i = 1$ ) are *i.i.d.* with  $\mathbb{P}(\tilde{p}_i \leq \frac{c_0}{1-s \cdot (1-c_0)}) = \mathbb{P}(L_i = 1) \leq \frac{c_0}{1-s \cdot (1-c_0)}$ , i.e., they stochastically dominate the uniform distribution and hence are valid p-values. Therefore, the condition of Theorem 3 holds so applying, as RESET does, Selective SeqStep+ with  $c = \frac{c_0}{1-s \cdot (1-c_0)}$  to these p-values controls the FDR at level  $\alpha$ . Note that the original formulation of Selective SeqStep+ is equivalent to Algorithm S1 since we identify the event  $\tilde{p}_i \leq \frac{c_0}{1-s \cdot (1-c_0)}$  with  $L_i = 1$  and  $\tilde{p}_i = 1$  with  $L_i = -1$ .  $\square$

**Theorem 2.** *Under Assumption 3 RESET controls the FDP at the user-specified threshold  $\alpha$  and confidence  $1 - \gamma$ .*

*Proof.* The proof of Theorem 1 shows that conditional on the learned scores  $\tilde{W}$  and the false null labels the labels  $L_i$  for  $i \in N$  with  $\tilde{L}_i = 1$  are distributed as *i.i.d.*  $\pm 1$  RVs, with  $\mathbb{P}(L_i = 1) \leq \frac{c_0}{1-s \cdot (1-c_0)}$ . Assuming for a moment that  $\mathbb{P}(L_i = 1) = \frac{c_0}{1-s \cdot (1-c_0)}$ , then RESET satisfies the assumption of the multiple decoy version of FDP-SD with  $c = \lambda = \frac{c_0}{1-s \cdot (1-c_0)}$  and therefore it controls the FDP at  $\alpha$  with confidence  $1 - \gamma$  (Section 4 of [40]). In the case that  $\mathbb{P}(L_i = 1) < \frac{c_0}{1-s \cdot (1-c_0)}$ , then the procedure is conservative with  $c = \lambda = \frac{c_0}{1-s \cdot (1-c_0)}$  and the proof in [40] follows without any modification.  $\square$

## S.4 Further implementation details of RESET

We point out some additional minor details regarding our implementation of RESET. We use the `randomxForest` package, `nnet` and `mgcv` to implement the random forest, two-layer neural network and generalized additive model in R, respectively. We used the default parameters for the random forest, the default parameters for the two-layer neural network and the default parameters for the generalized additive model (except we use `drop.intercept = TRUE`). If the number of side information variables used by RESET is  $\leq 3$ , a smoothing spline is fitted with `mgcv::s` otherwise a natural cubic spline is fitted using 5 degrees of freedom with `splines::ns` on each side information variable separately (for computational efficiency). For the use of GAM in RESET, we used `tryCatch` to switch to a random forest in the rare case that the GAM was not able to complete. Some real datasets contain p-values that are ‘zero’. Hence when we calculate  $W_i = |\Phi^{-1}(p_i)|$  for such p-values, we obtain `Inf` in R. We replace instances of `Inf` for the maximum real-valued score in the dataset. Lastly we used the default settings of RESET for *all* numerical and real data experiments unless otherwise stated in the main text.

## S.5 Further implementation details of Adaptive Knockoffs

There were some small differences between the implementations in the `adaptiveKnockoff` package in R and the code used in the original manuscript. Accordingly, we used the updated package version. We also fixed a minor bug, which pruned the candidate set  $\mathcal{S}$  *before* checking the estimated FDR is  $\leq \alpha$  — possibly missing out on a marginally larger discovery list. There are several parameters that may be set before applying the Adaptive Knockoff filters, e.g., the initial proportion of hypotheses revealed, `reveal_prop`. We used the same parameter settings in Simulation 1 as Simulation 1 in [44], and the same parameter settings in Simulation 2-4 as their Simulation 2 [44].

In the application to peptide detection, the primary scores  $W$  may be negative. Since Adaptive Knockoffs encodes the labels  $L$  by using the sign of the scores  $W$ , we shifted our peptide scores so that the minimum score was zero. For AdaKO EM, any peptide score  $\leq 10^{-3}$  was subsequently



assigned a zero score. Finally we used, `reveal_prop = 10%` which reveals the hypotheses that are less than or equal to the 10% of positive scoring hypotheses (which is the same setting used by the simulations). All other parameters were default.

## S.6 Further implementation details of the AdaPT methods

We implemented AdaPT using the `adaptMT` package in R. In Simulation 5 and 6, we used the same settings considered by the authors [33], i.e., we looked at AdaPT GAM in Simulation 5 and AdaPT GLMnet in Simulation 6 with the same parameters. Moreover, we considered AdaPT GLMnet in Simulation 5 with the same settings from Simulation 6, demonstrating the importance of selecting the correct working model. In the real datasets looked at by Zhang et al. [51], we used AdaPT GAM to fit a natural cubic spline using `splines::ns` with 5 degrees of freedom (knots chosen by default) on each side information variable. The use of natural cubic splines is a suggested option from the package documentation. There was an exception to this for the GTE<sub>x</sub> datasets, which flagged an error when we tried to apply the spline basis transformation on the ‘chromatin state of the SNP’. In this case, we applied no transformation to the affected side information variable. Zhang et al. mention that they employed a ‘5-degree for each dimension’, but it is not clear to us if they mean the degree of the piece-wise polynomials that make the spline, or the degrees of freedom of the spline. In the latter case, it is not clear how the knots are chosen, or how they overcame the error associated with the ‘chromatin state of the SNP’. Regardless, our results using AdaPT appear to be essentially the same. Moreover, Zhang et al. omits the application of AdaPT to the two fMRI datasets on account of the categorical side information variable used in these datasets. However, Chao and Fithian appear to still apply AdaPT<sub>g</sub> without problem, and so analogously we applied AdaPT as well. Lastly, in the gene-drug response data, we followed the same implementation by Lei and Fithian [33], which used AdaPT GLM and a collection of candidate side information transformations using `splines::ns` with degrees of freedom ranging from 6 to 10.

## S.7 Further implementation details of the AdaPT<sub>g</sub> methods

We implemented AdaPT<sub>g</sub> using the repository <https://github.com/patrickrchoo/adaptMT> which has all the same implementations as AdaPT while offering the ability to define asymmetric regions for mirroring the p-values. Accordingly, we followed the same implementation details as the previous section used by AdaPT and set the so-called ‘masking parameters’ as default.

## S.8 Further implementation details of AdaPT-GMM<sub>g</sub>

We implemented AdaPT-GMM<sub>g</sub> from the repository <https://github.com/patrickrchoo/AdaPTGMM>. In Simulations 5, we used the GAM filter (`model_type = ‘mgcv’`) to fit a smoothing spline using `mgcv::s` on the side information for the M-Step of the EM algorithm. In Simulation 6, we used a generalized linear model filter with regularization (`model_type = ‘glmnet’`) applied directly to the side information variables. For the real datasets used by Zhang et al. [51], we used the exact same implementation as Chao et al. from the file [https://github.com/patrickrchoo/AdaPTGMM\\_Experiments/blob/main/AdaFDR\\_experiments/run\\_all\\_exp.R](https://github.com/patrickrchoo/AdaPTGMM_Experiments/blob/main/AdaFDR_experiments/run_all_exp.R). In the gene-drug response data, since only one-dimensional side information is used, we copied the parameters selected from the previous real datasets that also considered just one-dimensional side information.

## S.9 Further implementation details of ZAP

We used the default parameters of `zap_asymp` from the ZAP package <https://github.com/dmhleung/zap>. In all simulations and real data experiments, we considered a natural cubic spline basis expansion on each side information variable with six degrees of freedom using `splines::ns`. This choice was based on their own analysis on two of the real datasets that we consider here, Airway and Bottomly. The exception was in Simulation 6, where we directly used all 100 side information variables rather than applying a spline basis expansion on each of them. In Simulation 5 and 6, we used the test statistics obtained as input, while in the real data experiments we converted the p-values to z-values by using the transformation  $\pm\Phi^{-1}(p_i/2)$  on each p-value  $p_i$  where the signs are chosen *i.i.d.* uniformly.

## S.10 Further implementation details of AdaFDR

We applied AdaFDR using the `method.adafdr.test` function from the AdaFDR package <https://github.com/martinjzhang/adafdr>. We note that installation of the package required setting up a separate conda environment so that we could install an older version of Python (v3.6.13). This was because recent versions of Python do not support PyTorch v1.4.0, a requirement of the AdaFDR package `setup.py` file.

We used the exact same parameters in the vignettes <https://github.com/martinjzhang/AdaFDRpaper/tree/master/vignettes> to implement AdaFDR on the 10 datasets that Zhang et al. look at. Interestingly, the two fMRI datasets only consider the Brodmann label as the side information. We tried using all the available side information, but the statistical power was worse (data not shown). In the gene-drug response data, we used AdaFDR with `fast_mode = False`. This is in accordance to the discussion from their paper that the fast version of AdaFDR is recommended when few discoveries are expected or if the number of hypotheses is small (which is not the case for both of the gene-drug response datasets).

## S.11 Computer specifications for computation times

Computation times were calculated using an M1 Mac Studio with 20-core CPU and 128GB RAM.

## S.12 Data preparation and searching with HEK293 data

We downloaded the human proteome (UP000005640, downloaded on 2023/09/23 from UniProt) and prepared a target peptide database along with 5 randomly shuffled decoy peptide databases using Tide-index within the Crux Toolkit v4.1.6809338 [29, 43] with all options set to default. An output containing the target and decoy peptide pairs are conveniently provided using the `--peptide-list T` option in Tide-index. Each of the RAW 24 HEK293 spectrum files [9] were converted to mzML format using MSConvert 3.0.22314 with the vendor peak-picking filter using the default settings. For each of the 5 decoy databases, we searched each spectrum from the combined 24 mzML spectrum files against the combined target-decoy peptide database using Tide-search [15], using the options `--top-match 1 --auto-precursor-window warn --auto-mz-bin-width warn --concat T`. The resulting search files were then converted to so-called pin files using the `make-pin` function in Crux. Each row in the pin files correspond to the optimal peptide-spectrum match (PSM) for each spectrum, the primary score for quantifying this match, called *XCorr* scores, and a collection of auxiliary information regarding the PSM.

Search algorithms like the one above are typically ‘spectrum-centric’, meaning that for each spectrum, we look for the best matching database peptide, as oppose to the other way round.

Side Information	Description
deltCn	The difference between the XCorr score of the two top ranked PSMs with respect to the combined database, divided by maximum of the top PSM XCorr score and 1
PepLen	The length of the matched peptide, in residues
Charge	The charge of the precursor ion (ranging from +1 to + 5)
lnNumSP	The natural logarithm of the number of database peptides within the specified precursor range
dm	The difference between the calculated and observed mass
absdM	The absolute value of the difference between the calculated and observed mass

Table S4: **List of described side information used by HEK293 data.** The list of side information used by RESET and Adaptive Knockoffs in the HEK293 data, adapted from <https://crux.ms/file-formats/features.html>. Note that the Charge state is represented as a one-hot vector, where we left out a Charge state of +1 (due to linearity, since the one-hot vector sums to one).

Consequently, the same database peptide may be matched multiple times with different scores, or have no match at all. Hence for each target peptide, we define  $Z_i$  as the maximum XCorr score of all the PSMs associated to that target peptide. Similarly for each decoy peptide, we define  $\tilde{Z}_i$  as the maximum XCorr score of all the PSMs associated to that decoy peptide. For target or decoy peptides that do not appear in the pin file, they get a score of  $-\infty$ . Then we compete each target and its corresponding paired decoy by recording the winning score  $W_i = Z_i \vee \tilde{Z}_i$  along with the label  $L_i = \text{sign}(Z_i - \tilde{Z}_i)$ , randomly breaking any ties. Peptides with a winning score of  $-\infty$ , indicating that neither the target or its paired decoy are in the pin file, are thrown out. We assign each winning peptide the side information defined as the auxiliary information  $\mathbf{x}_i$  of the underlying PSM that had the XCorr score of  $W_i$ . The side information that was subsequently used by RESET and Adaptive Knockoffs is given in Table S4.

### S.13 Estimating the computation times of Adaptive Knockoffs

Running Adaptive Knockoffs (AdaKO) on all peptide datasets would be infeasible. Therefore, we resorted to estimating its runtimes by considering the time it took to complete a single iteration that determines which hypothesis to reveal next, and multiplying this value by the estimated number of iterations before the procedure stops.

Since the time it takes a single iteration depends on the number of hypotheses that were already revealed, we took different such measurements as we varied this number, and averaged them. Specifically, as AdaKO does, we first revealed the labels that were scored less than or equal to the 10% quantile of non-zero scoring hypotheses, and recorded the time it takes for a single iteration from this point. To be clear, the revealed labels thus *includes* those zero-scoring hypotheses since they will be less than this score cutoff — it is only the 10% quantile that considers the non-zero scoring hypotheses. Then we took similar measurements by increasing the ‘10%’ value, in 10% increments, up to a value of ‘10k%’ where we define  $k$  next.

We chose the value of  $k$  so that the proportion of revealed labels,  $10k\%$ , estimates the number of revealed labels when AdaKO terminates at the 1% FDR level. That way, the  $k$  times should provide an accurate sample of the number single iteration times across all of AdaKO’s iterations until it terminates. Of course, we are unable to compute when Adaptive Knockoffs might terminate, so we estimated this using the value  $q$ , the number of target and decoy peptides that scored above the 1% FDR cutoff using RESET Ensemble. Then we defined  $k = \lfloor (m - q)/m \cdot 10 \rfloor$ , where  $m$  is the total number of hypotheses (peptides) considered by Adaptive Knockoffs. We estimated the

runtime by

$$\bar{t}_k \cdot (m' - q),$$

where  $\bar{t}_k$  is the average of the  $k$  measured single-iteration times, and  $m'$  is the number of labels that are yet to be revealed at the start of AdaKO’s iterations, i.e., the number of labels with scores above the 10% quantile of non-zero scoring hypotheses. Thus the value  $m' - q$  is our estimate of the number of iterations until Adaptive Knockoffs stop.

In Section 5.2.2, we considered 10 repeated applications of RESET Ensemble, varying RESET Ensemble’s internal seed. In this case, we define  $\bar{\ell}$  as the average of the number of winning target and decoy peptides above the cutoff over each application.

## S.14 Data preparation and searching with PRIDE-20 data

We followed the preparation and searching outlined in [18]. The only difference is that we used an updated version of the Crux toolkit. We provide the following brief description for the reader’s convenience. Twenty spectrum files and protein databases from separate projects, referred to as the PRIDE-20 dataset, were downloaded. Tide-index was used to prepare the target peptide database along with 10 randomly shuffled decoy peptide databases for each of the 20 spectrum files. Tide-search was used to search each spectrum file against the 10 combined target-decoy databases using two modes: ‘narrow’ and ‘open’ search options as they outline. Briefly a ‘narrow’ search, which is the default search mode, only searches each spectrum in the spectrum file against peptides in the target-decoy database that have a theoretical mass within a small tolerance of the sample peptide’s mass that generated the experimental spectrum. On the other hand, an ‘open’ search makes this mass-tolerance larger so that a spectrum may match with a peptide with a completely different mass. This is desirable at times, since sample peptides can undergo *post-translational modifications* which modify the mass of the peptide and therefore the experimental spectrum. Hence when searching in an ‘open’ mode, the modified spectrum may still be correctly matched. The search files were then converted to pin files using the make-pin function in Crux and subsequently filtered for the top 1 (the optimal) peptide-spectrum match for each spectrum.

For each spectrum file and search type, we obtained the triples  $(L, W, \mathbf{x})$  in the following way. For each spectrum file that had no modifications (we explain this in more detail next), we proceeded essentially in the same way as in Section S.12. That is, for each peptide in the pin file, we define  $Z_i$  (if a target peptide) or  $\tilde{Z}_i$  (if a decoy peptide) as the maximum *Tailor* score of all the PSMs associated to the target peptide [47]. Here we are using the more sensitive *Tailor* scores and relegate the *XCorr* scores as one of the side information variables. Then we compete each target and its corresponding paired decoy in the same way as Section S.12, to obtain the triple  $(L_i, W_i, \mathbf{x}_i)$  where the side information  $\mathbf{x}_i$  is obtained from the auxiliary information of the underlying PSM that had the *Tailor* score of  $W_i$ . A description of the side information used is given in Table S5.

We next consider spectrum files that were searched with variable modifications (`---auto-modifications T`). Here we need to make a slight adjustment to account for some dependency within the data. Specifically, using variable modifications creates several ‘copies’ of the peptides in the target-decoy database that are distinguished only by slight alterations to the mass of some of the amino acids. As an example, PEPTIDE may generate the following ‘copies’: PE[16]PTIDE, PEPTIDE[16] and PE[16]PTIDE[16], where [16] indicates an increase of 16 Daltons to the amino acid on the left. Consequently, each of these peptides are usually correlated in the data — i.e., if one of these peptides is scored high, than usually they all are. Hence in order to satisfy Assumption 3, we follow the protocol outlined in [18]. That is, we identify all the copies as being the same peptide, ‘PEPTIDE’, with each of the variable modifications ignored. Then we proceed with the same steps as the above paragraph, by determining the maximum score associated with PEPTIDE and recording

Side Information	Description
deltLCn	The difference between the XCorr score of the top scoring PSM and the fifth/last ranked PSM with respect to the combined database, divided by the maximum of the top PSM’s XCorr score and 1
deltCn	The difference between the XCorr score of the two top ranked PSMs with respect to the combined database, divided by maximum of the top PSM XCorr score and 1
Xcorr	The SEQUEST cross-correlation PSM score
PepLen	The length of the matched peptide, in residues
Charge	The charge of the precursor ion (ranging from +1 to + 5)
lnNumSP	The natural logarithm of the number of database peptides within the specified precursor range
dm	The difference between the calculated and observed mass
absdM	The absolute value of the difference between the calculated and observed mass

Table S5: **List of described side information used by PRIDE-20 data.** The list of side information used by RESET and Adaptive Knockoffs in the PRIDE-20 data, adapted from <https://crux.ms/file-formats/features.html>. Note that the Charge state is represented as a one-hot vector, where we left out a Charge state of +1 (due to linearity, since the one-hot vector sums to one). XCorr is used as side information since we define  $W$  in terms of Tailor scores here instead.

it as  $Z_i$  (or  $\tilde{Z}_i$  if it is a decoy). We define the labels, winning scores and side information in the same way to obtain our triplets  $(L, W, \mathbf{x}_i)$ .

Due to runtime considerations, we used 13 of the smallest narrow search files to assess Adaptive Knockoff’s power as described in Section 5.2.2 of the manuscript, and only one of the 10 target-decoy databases. To fairly compare with Adaptive Knockoffs, we used the same target-decoy databases for RESET ensemble. All 20 spectrum files and all 10 target-decoy databases for each spectrum file were used in the comparison of RESET ensemble and FDP-SD while controlling the FDP.

### S.15 Brief justification of the assumptions used with HEK293 and PRIDE-20 datasets

A standard assumption of the mass spectrometry literature, which is also empirically validated, is that the label  $L_i$ , indicating whether an incorrect target or its decoy scored higher, is uniformly  $\pm 1$  independently of all other target-decoy pairs and scores [21, 39]. RESET *additionally* requires this statement to be true if we further condition on the side information. This is obviously true for some side information variables which are constant between the target and corresponding decoys — e.g., PepLen, Charge, lnNumSP, dm, absdM. The other side information variables are score-related — e.g., Xcorr, deltCn and deltLCn, and so conditioning on them assumes no more than the ‘standard assumption’. Hence, we believe Assumption 3 with  $P(L_i = 1) = c_0 = 1/2$  to be reasonably satisfied.

### S.16 Preparation of data with p-values

Each of the 10 datasets from Zhang et al. were downloaded from [https://github.com/patrickrchoo/AdaPTGMM\\_Experiments/tree/main/AdaFDR\\_experiments/data\\_files](https://github.com/patrickrchoo/AdaPTGMM_Experiments/tree/main/AdaFDR_experiments/data_files), containing the p-value and side information pairs,  $(p, \mathbf{x})$ . All pairs were then used to report a list of discoveries by each p-value based method with the following exceptions. In the RNA-seq datasets, Airway, Bottomly and Pasilla, there exists ‘spikes’ of high p-values. These ‘spikes’ concentrate in certain regions of the side information, i.e., when the log-normalized gene counts are low. Hence we removed those p-values with log-normalized gene counts that were less than zero. Figure S1 show the histograms

of the p-values before and after this removal. The gene-drug response data was obtained from the adaptMT package.

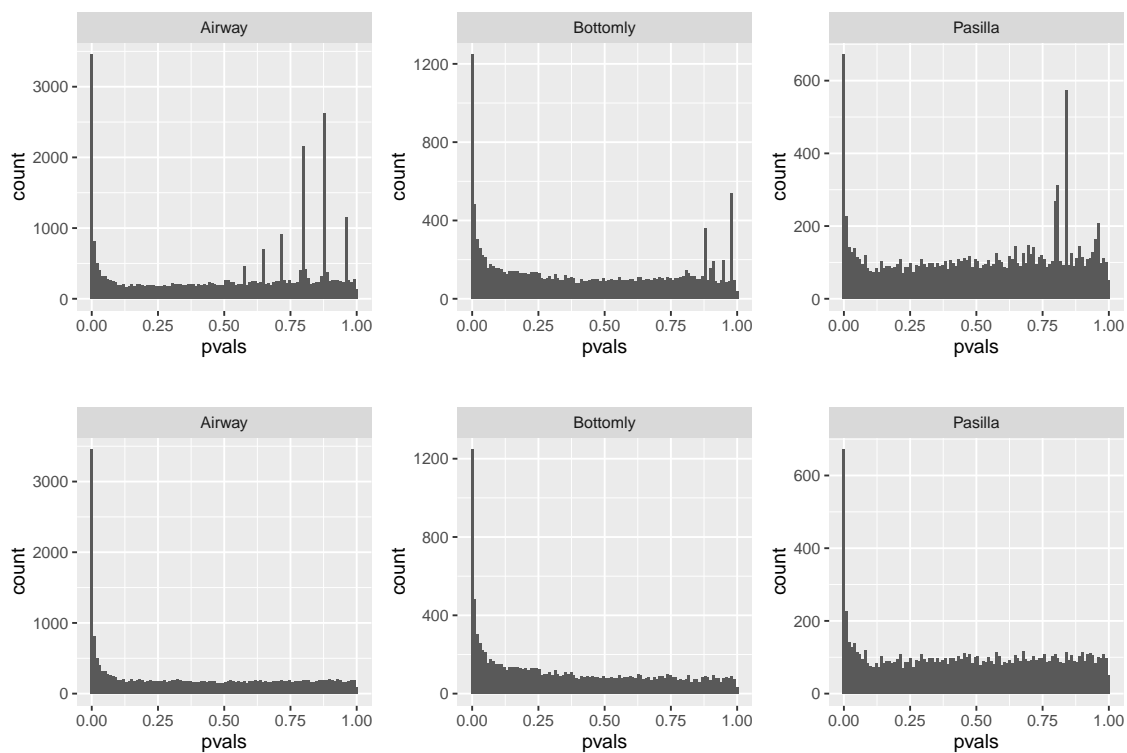


Figure S1: **Histograms of p-values in the RNA-seq data before and after p-value removal.** Top row: the original histograms of the p-values. Bottom row: the corresponding histograms after removal of the p-values associated with low counts.

## S.17 Tables

Project ID	Method	Estimated Time	Actual Time	Discoveries
PXD002470	AdaKO EM	0.58	1.17	300
	AdaKO GAM	0.03	0.08	272
	AdaKO LR	0.07	0.14	483
	AdaKO RF	7.50	9.04	488
	TDC	-	-	455
PXD006856	AdaKO EM	24.72	59.80	0
	AdaKO GAM	0.80	2.17	379
	AdaKO LR	3.67	4.63	428
	AdaKO RF	427.01	486.70	421
	TDC	-	-	425
PXD008920	AdaKO EM	33.81	48.63	8485
	AdaKO GAM	0.95	2.39	8443
	AdaKO LR	2.98	6.11	9143
	AdaKO RF	250.66	270.67	9352
	TDC	-	-	9086
PXD008996	AdaKO EM	119.73	188.54	7464
	AdaKO GAM	3.39	7.55	7958
	AdaKO LR	18.77	20.18	8481
	AdaKO RF	1430.16	1626.96	8625
	TDC	-	-	8413
PXD010504	AdaKO EM	134.07	185.59	459
	AdaKO GAM	4.03	5.11	1358
	AdaKO LR	9.25	11.37	1585
	AdaKO RF	2134.38	2420.31	1626
	TDC	-	-	1551
PXD012528	AdaKO EM	202.99	241.66	0
	AdaKO GAM	6.37	8.34	239
	AdaKO LR	13.57	16.34	314
	AdaKO RF	3769.54	4143.21	405
	TDC	-	-	342
PXD012611	AdaKO EM	4.79	7.59	2850
	AdaKO GAM	0.15	0.26	3152
	AdaKO LR	0.62	0.98	3250
	AdaKO RF	43.53	47.01	3262
	TDC	-	-	3260
PXD013274	AdaKO EM	34.65	49.52	14025
	AdaKO GAM	0.81	1.70	14271
	AdaKO LR	4.59	3.92	14791
	AdaKO RF	205.10	248.82	14765
	TDC	-	-	14769.0
PXD016724	AdaKO EM	499.32	598.31	3617
	AdaKO GAM	13.76	24.01	3802
	AdaKO LR	36.84	58.90	4536
	AdaKO RF	8070.09	8882.65	4809

	TDC	-	-	4745
PXD019186	AdaKO EM	247.15	389.51	0
	AdaKO GAM	7.04	13.49	1020
	AdaKO LR	34.77	30.35	942
	AdaKO RF	4143.83	4427.20	1217
	TDC	-	-	912
PXD022257	AdaKO EM	151.82	244.22	1619
	AdaKO GAM	15.50	9.94	1918
	AdaKO LR	12.34	23.81	2500
	AdaKO RF	2475.32	2638.35	2501
	TDC	-	-	2509
PXD023571	AdaKO EM	30.23	43.86	1030
	AdaKO GAM	3.04	4.40	1743
	AdaKO LR	2.92	10.34	0
	AdaKO RF	437.75	474.17	2161
	TDC	-	-	1505
PXD026895	AdaKO EM	62.89	85.62	3255
	AdaKO GAM	8.94	4.94	3676
	AdaKO LR	10.02	12.04	4044
	AdaKO RF	847.23	835.02	4047
	TDC	-	-	3980.0

Table S6: **The number of discoveries and computations times for 13 of the PRIDE-20 dataset at the 1% FDR level.** We calculated the number of discoveries at the 1% FDR using each method of Adaptive Knockoffs and TDC. We also computed computation times for Adaptive Knockoffs (in minutes). We used both the actual times and the estimated times according to Section S.13.



## S.18 Figures

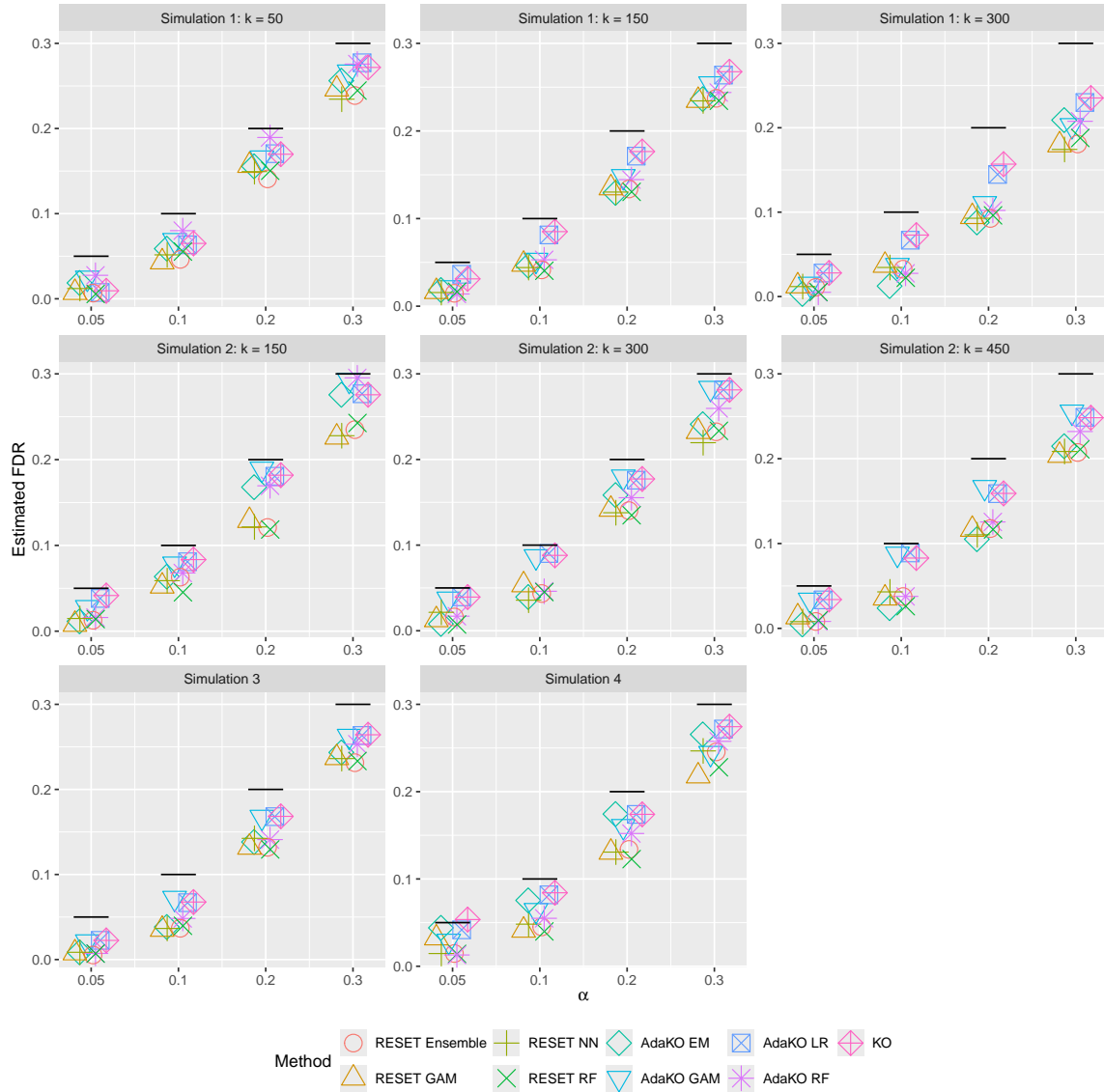


Figure S2: **Estimated FDR of each method in numerical simulations.** Each panel plots the estimated FDR for each method at FDR thresholds ranging from 5% to 30%. The first row corresponds to Simulation 1 with three values of  $k \in \{50, 150, 300\}$ , the second row corresponds to Simulation 2 with three values of  $k \in \{150, 300, 450\}$ , and the last row corresponds to Simulation 3 and 4. For readability, the points are jittered in the horizontal direction.

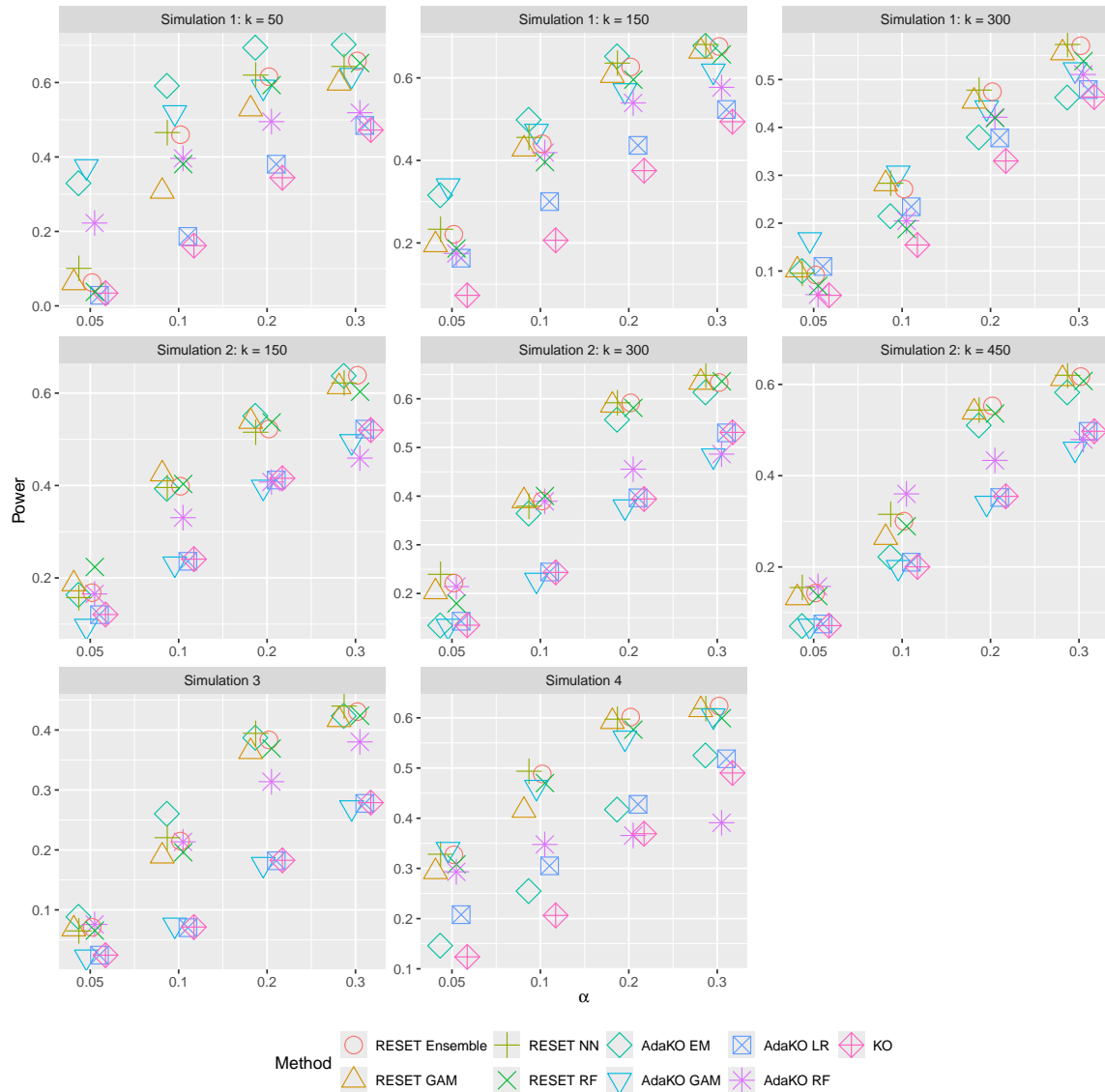


Figure S3: **Estimated power of each method in numerical simulations.** Each panel plots the power for each method at FDR thresholds ranging from 5% to 30%. The first row corresponds to Simulation 1 with three values of  $k \in \{50, 150, 300\}$ , the second row corresponds to Simulation 2 with three values of  $k \in \{150, 300, 450\}$ , and the last row corresponds to Simulation 3 and 4. For readability, the points are jittered in the horizontal direction. A description of the AdaKO methods and KO can be found in Section 2.